

ZENTRUM  
FÜR BIODIVERSITÄT UND NACHHALTIGE LANDNUTZUNG  
– CENTRE OF BIODIVERSITY AND SUSTAINABLE LAND USE –

---

# Xylem anatomy and branch embolism resistance of Sumatran rainforest trees

---

Master's Thesis submitted in partial fulfillment  
of the requirements for the degree  
"Master of Science" (M.Sc.)  
in the study programme  
"Biodiversity, Ecology and Evolution"  
at the Georg-August Universität Göttingen  
prepared at the

Albrecht- von- Haller Institute for Plant Sciences  
Department for Plant Ecology and Ecosystems Research

Submitted by

BSc, Kyra May Ute Zembold

Göttingen, April 2019

First reviewer: Prof. Dr. Christoph Leuschner

Second reviewer: Prof. Dr. Bernhard Schuldt

Date of announcement of the Master's Thesis: 31.10.2018

Date of submission of the Master's Thesis: 08.04.2019

---

## Content

Abstract.....	iv
1. Introduction.....	1
1.1 Sap flow and the xylem .....	2
1.2 Drought resistance of tropical rainforest trees .....	4
1.3 Aims and hypotheses .....	6
2. Methods.....	7
2.1 Study area and investigated species .....	7
2.2 Sample collection .....	7
2.3 Maximum vessel length.....	7
2.4 Xylem vulnerability to cavitation.....	9
2.5 Xylem anatomy and potential conductivity .....	10
2.6 Stand characteristics .....	11
2.7 Data analysis.....	12
3. Results .....	13
3.1 Tree structural traits and growth .....	13
3.2 Xylem anatomy .....	15
3.3 Vulnerability curves .....	17
3.4 Associations among the investigated traits.....	19
4. Discussion .....	23
4.1 Predictors for xylem safety .....	23
4.2 Efficiency/ safety trade-off .....	26
4.3 Constraints of the study.....	26
4.4 Implications for future species composition .....	27
5. Conclusion.....	28
Acknowledgement .....	I
References.....	II
Appendix .....	XV

## Tables

Table 1: Characteristics of the eight investigated species.....	8
Table 2: Pearson correlation for Xylem vulnerability and 11 relevant tree structural and xylem anatomical traits.....	22

## Figures

Figure 1: Feedback cycles resulting from accelerated tree mortality.....	1
Figure 2: Anatomy of the xylem and interconduit pits.....	3
Figure 3: Tree structural traits (H and WD).....	13
Figure 4: Development of the aboveground biomass (AGB).....	14
Figure 5: Xylem anatomy.....	16
Figure 6: Vulnerability curves.....	18
Figure 7: Wood density (WD) in relation to xylem anatomical traits.....	19
Figure 8: Tree height (H) in relation to vessel diameter.....	20
Figure 9: $P_{50}$ in relation to its four expected main predictors.....	21

## Abbreviations

	Unit	Description
AGB	kg	Above ground biomass
$A_{\text{lumen}}$	$\text{mm}^2$	Total vessel lumen area
$A_{\text{lumen}} : A_{\text{xylem}}$	%	Relative vessel lumen area
$A_{\text{xylem}}$	$\text{mm}^2$	Total xylem area
D	$\mu\text{m}$	Mean vessel diameter
DBH	cm	Stem diameter at breast height (1.3 m)
$D_h$	$\mu\text{m}$	Hydraulically weighted mean vessel diameter
$D_{\text{max}}$	$\mu\text{m}$	Maximum vessel diameter
H	m	Tree height
$H_{\text{max}}$	m	Maximum tree height (tallest individual on plot)
$K_{\text{init}}$	$\text{kg m}^{-1} \text{MPa}^{-1} \text{s}^{-1}$	Initial conductivity (with embolized vessels)
$K_{\text{max}}$	$\text{kg m}^{-1} \text{MPa}^{-1} \text{s}^{-1}$	Maximum conductivity
$K_p$	$\text{kg m}^{-1} \text{MPa}^{-1} \text{s}^{-1}$	Potential conductivity
MVL	cm	Maximum vessel length
$P_{50}$	MPa	Water potential at 50% loss of conductivity
$\Psi$	MPa	Water potential
PLC	%	Percentage loss of conductivity
VD	$\text{n mm}^{-2}$	Vessel density
WD	$\text{g cm}^{-3}$	Wood density

## **Abstract**

Recent shifts in precipitation regimes and rising temperatures have caused global drought-induced tree mortality in forest ecosystems. Hydraulic failure is the primary driver of plant mortality during drought. Hence, xylem safety is a key parameter to understand mortality patterns. In this study, eight tree species from a perhumid tropical rainforest on Sumatra (Indonesia) were sampled and tested for their xylem vulnerability to drought-induced embolisms with the bench dehydration method. The water potential at 50% loss of hydraulic conductivity ( $P_{50}$ ) of each species was taken as a comparative measure for xylem vulnerability. Additionally, tree height and wood density as well as xylem anatomical traits and growth performance were analyzed to correlate potential predictors with xylem vulnerability. The proposed predictors did not show a significant correlation with xylem vulnerability. Therefore, the relationship between xylem vulnerability and vessel anatomy remains unclear, suggesting that the main determinant of xylem safety was not assessed in this study or that limits in methodology hindered the compilation of a robust data set. Moreover, complex traits like wood density and tree height appear to be non-reliable predictors of xylem vulnerability. None of the investigated species showed a high conductivity and a high xylem safety, suggesting a trade-off between xylem safety and efficiency. However, three of the eight species showed a low efficiency and a low safety. We suppose that the perhumid climate causes a weak selective pressure towards xylem safety. Further, we report xylem anatomical differences among Sumatran rainforests trees, which were shown to determine species distribution in regard to different moisture regimes. This implies that altering precipitation patterns in the course of global climate change will presumably affect the distribution of Sumatran forest trees.

## 1. Introduction

Climatic stress as a cause of major tree diebacks gained increasing importance over the past decades (Engelbrecht 2012; Allen et al. 2010 and 2015). Prolonged drought events and exceptional heat waves have led to rising tree mortality in globally distributed forest-ecosystems (Ma et al. 2011; Rouvinen et al. 2002; van Mantgem and Stephenson 2007), including tropical rainforests in Amazonia and Borneo (Phillips et al. 2010). These extreme weather events are a concomitant phenomenon of the ongoing global climate change and will most likely intensify in the future (IPCC 2014). The subsequent forest diebacks entail a variety of geochemical and ecological consequences. The expected CO<sub>2</sub>-release will fortify the global climate change and eventually lead to a remarkable alteration in atmosphere composition, as woody biomass contains about 60% of the atmospheric carbon (Denman et al. 2007). This is especially true for tropical rainforests, which are highly productive and hold approximately half of the global biomass (Hunter et al. 2013; Pan et al. 2013). Hence, they are an effective carbon sink at the current state (Bonan 2008), but drought-induced diebacks might turn them into a net carbon source within this century (Clark 2004; Lewis 2006). This process will contribute to a feedback cycle, as illustrated in Figure 1.

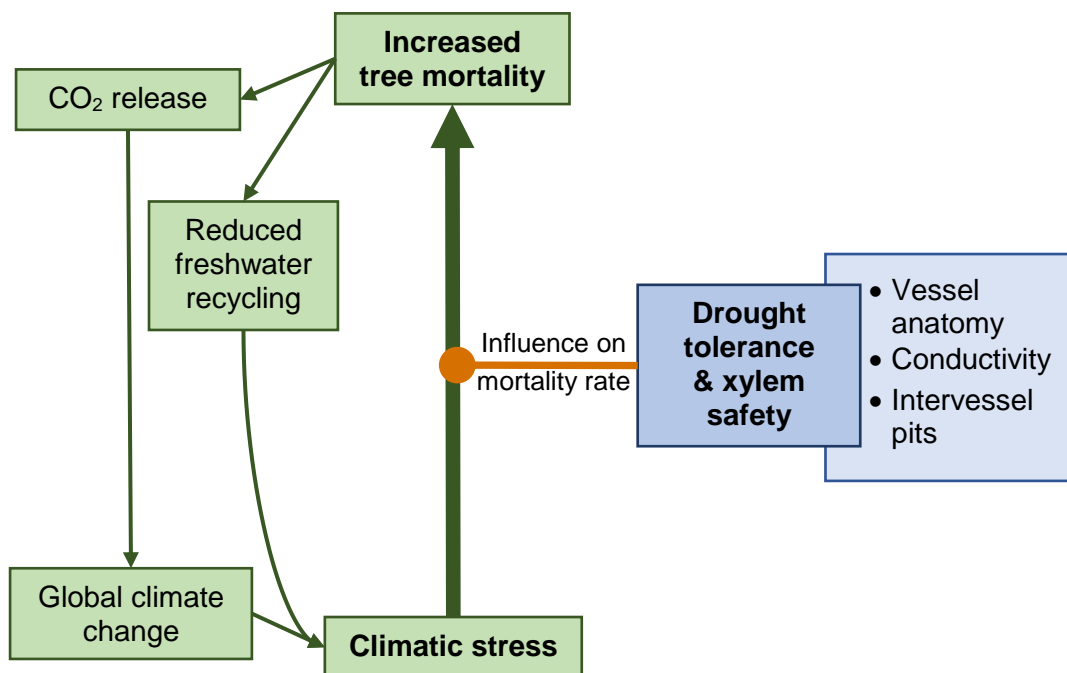


Figure 1: Feedback cycles resulting from accelerated tree mortality (green arrows). Carbon release contributes to global climate change, which causes droughts through decreased precipitation and increased temperatures. The reduced freshwater recycling, driven by the removal of plant cover, triggers water deficits as well. A key determinant for mortality rates during climatic stress is the inherent drought resistance of tree species (orange arrow). Drought tolerance is influenced by xylem safety, which might depend on traits like vessel anatomy, conductivity and intervessel pit structures (blue box).

Furthermore, the terrestrial plant cover plays a crucial role in hydrological circulation (Rind 2013). Through storing and transpiring water, forests are an important regulator in regional and global water cycles (Roberts 2009; Bond et al. 2008) and their removal leads to a decrease in evapotranspiration and thus a decrease in rainfall, whereas the water runoff increases (D'Almeida et al. 2007). These changes reduce the recycling of freshwater resources, ultimately resulting in more pronounced water deficits in the affected regions (Figure 1). Finally, the biodiversity in areas with extensive forest diebacks is substantially lost (Giam 2017). As plants compose the base of all terrestrial ecosystems, the dieback of plant cover means a complete destruction of habitat structures as well as nutrition supply for all higher trophic groups (Ebeling et al. 2018; Scherber et al. 2010).

These aspects raise concern about the fate of forest biomes in view of globally changing climate. Hence, the prediction of tree mortality under drought conditions and a more profound scientific knowledge of the underlying mechanisms appear crucial to model future dynamics in tropical rainforests, as well as taking action to handle approaching developments (Meir et al. 2015).

### **1.1 Sap flow and the xylem**

It has been demonstrated, that hydraulic failure is the main driver of drought-induced mortality in trees (Rowland et al. 2015). The resistance of their water transport system (xylem) towards gas embolisms was found to be the best predictor for mortality patterns (Anderegg et al. 2016; Powell et al. 2017). The xylem in broad-leafed trees is a conduit network that consists of a multitude of connected vessel elements (Tyree and Zimmermann 2002). Water is absorbed through the roots and transported to the leaves, where it is used for physiological processes and finally transpired back to the atmosphere. Single conduit elements form a continuous vessel, as their end walls are fully or partially dissolved (see Figure 2A and C). Additionally, these vessels are laterally interconnected via bordered pits (Choat et al. 2008, Figure 2B and D). This network holds a constant water column and the mechanism of water transport is described by the cohesion-tension theory (Boehm 1893; Dixon and Joly 1894). It remains the most widespread concept to explain the upward water movement in xylem conduits (Kim et al. 2014; Tyree 2003). According to the cohesion-tension theory, the water transport is propelled by cohesion and adhesion forces among single water molecules and the cell wall. As water molecules evaporate through the stomata on the leaf foliage, the air-water interface develops a negative curvature, but the inherent surface tension of water strives to form a straight plain, consequently pulling on the entire water column (Tyree and Sperry 1989). This negative pressure (water potential) is transmitted throughout the vertical water volume in the vessels, leading to pressure values of -1 to -2 MPa under non-drought conditions. Under these

conditions, the water is in a metastable state and the water inside the vessels would naturally turn into vapor to be in a thermodynamic equilibrium. But due to hydrogen bonding, the cohesion between single water molecules protracts the change into gas phase (Tyree and Sperry 1989). This mechanism allows the transport of large water quantities, in spite of rigid cell walls that prohibit active movement and without a high metabolic input (Tyree 2003).

However, this transport system fails if gas voids enter the xylem system, because gas embolisms disrupt the water column and therefore break the water flow (Cochard 2006). Air can enter a vessel through the pit membranes (Choat et al. 2008; Rockwell et al. 2014) or leaks in the cell wall, if the tension in the vessel lumen becomes too strong in the course of desiccation. As soon as air enters the vessel, it nucleates further cavitation (Cochard 2006). Spontaneous cavitation without a nucleation event has been rendered unlikely, because the required water potential would be too low (Brown 2013; Nardini et al. 2018).

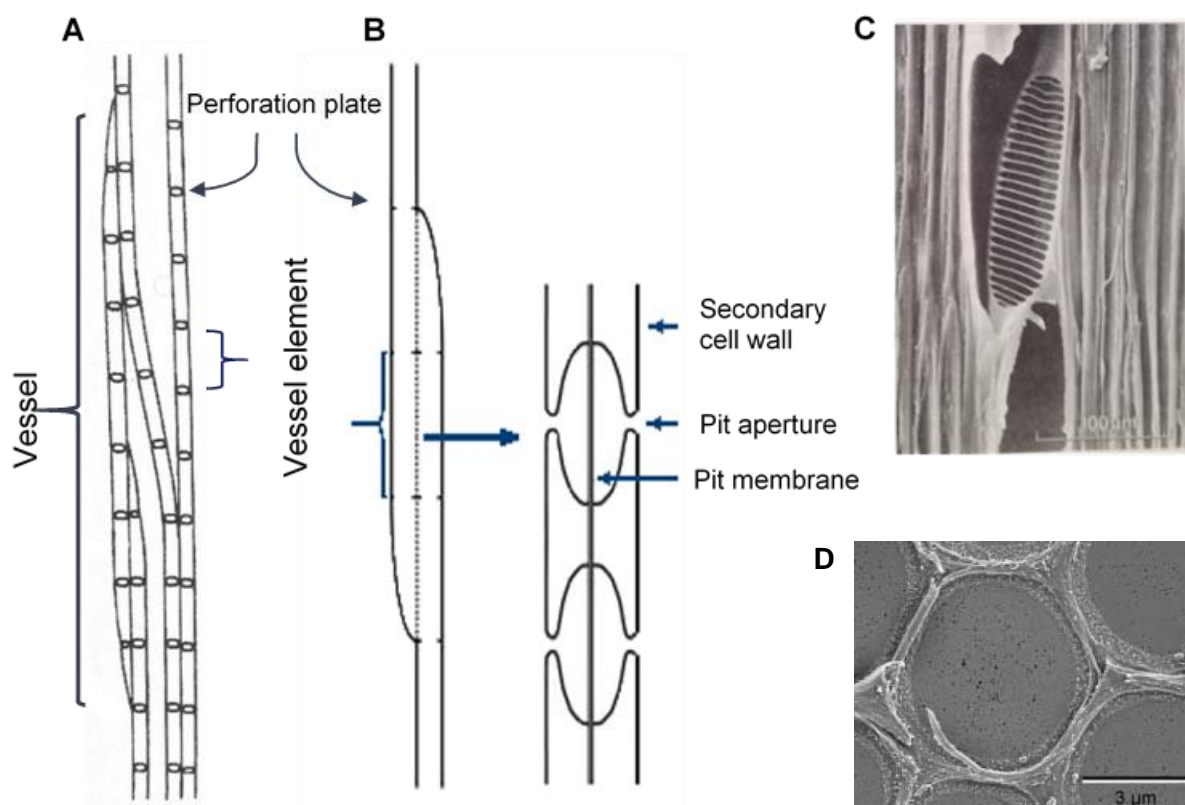


Figure 2: Anatomy of the xylem and interconduit pits. A: The vessel matrix consists of multiple vessel elements, that form the conduits. These vessels are laterally connected at the overlapping areas (amended from Tyree and Zimmermann, 2002). B: Two vessels are connected via a pit membrane with bordered pits. *Right* The overarching secondary cell wall provides mechanical strength while maximizing the conductive area at the pit membranes (Amended from Choat et al., 2008). C: Scalariform perforation plate between two vessel elements. Adjacent to the vessel multiple tracheids are visible (Scanning electron micrograph, Tyree, Zimmermann 2002). D: Pit membranes showing pores (Scanning electron micrograph, Choat et al. 2008)

The tree can compensate a limited number of cavitation events via redundancy within the vessel matrix (see Fig. 2A), but eventually a high number of embolisms can lead to hydraulic failure and cause irreversible damages in the plant. A common measure for xylem vulnerability towards cavitation is the  $P_{50}$  value, which represents the water potential at which 50% of xylem conductivity is lost due to embolisms (Pérez-Harguindeguy et al. 2013; Choat et al. 2012).

According to the Hagen-Poiseuille equation, the hydraulic conductivity of a conduit increases with the fourth power of vessel diameter (Tyree and Zimmermann 2002). Hence, the water transport in few large vessels is more efficient than in many small vessels. But large vessels have been found to bear a higher risk of cavitation (Sperry and Tyree 1988; Tyree and Sperry 1989) and a xylem system with many small vessels can profit from higher redundancy in case of embolisms (Tyree and Zimmermann 2002). Consequently, trees are facing an essential trade-off between xylem safety and efficiency. This is mirrored in the common finding, that vessel diameter and vessel density correlate negatively (Zanne et al. 2010; Guzman et al. 2016; van der Sande et al. 2019). However, some studies report a low correlation between xylem efficiency and safety, which is caused by a considerable number of species, that have a low efficiency and safety (Gleason et al. 2016). Another major aspect of this trade-off is that the resistivity of end walls and intervessel pits reduces conductivity and thus efficiency (Sperry et al. 2008). But air or water vapor does not easily pass intervessel pits (Choat et al. 2008), so short vessels tend to limit the cavitation to the area of its occurrence, therefore enhancing safety (Comstock and Sperry 2000). Indeed, the total pit area (Wheeler et al. 2005) as well as the thickness and porosity of pit membranes (Li et al. 2016; Jansen et al. 2009) have been found to be very closely associated with xylem vulnerability, indicating that pit-related traits might be one of the best predictors for xylem vulnerability.

## **1.2 Drought resistance of tropical rainforest trees**

Tropical rainforests cover only about 7% of the land's surface, but they hold the highest number of species amongst all terrestrial biomes (Brown 2014; Groombridge and Jenkins 2002). This great biodiversity is strongly dependent on the rich moisture status of the habitat and water availability is a key determinant of species distribution in tropical rainforests (Cosme et al. 2017; Engelbrecht et al. 2007), with a higher impact than light or nutrient availability (Gaviria et al. 2017). Experiments with artificial drought have reported a decrease of 20% in standing biomass after only 7 years of low rainfall (da Costa et al. 2010). After 13 years this doubled to a loss of 40% (Rowland et al. 2015). In addition, mortality rates are not evenly distributed across functional groups. Large trees with high stem diameters have been shown to suffer from higher mortality rates than thinner trees (da Costa et al. 2010; Phillips et al. 2010; Zhang et al. 2009), which is mainly caused by hydraulic deterioration (Bennett et al. 2015; Rowland

et al. 2015). As diameter and tree height scale positively, tall trees can be assumed to be more vulnerable to drought-induced mortality. Additionally, tree height scales with a physiological demand for a higher water supply (Hietz et al. 2016), which is in line with studies, that report larger vessel diameters in tall trees (Zach et al. 2010; Olson et al. 2014). Emergent trees play a crucial role in the complex layered structure of rainforest canopies, as they provide shade and increased air humidity for lower canopy layers. Specialized species in those lower layers depend on their particular microclimate regarding parameters like solar radiance and air humidity (Kitajima et al. 2005) and the disappearance of tall trees could lead to further damage in smaller trees and understorey (Nepstad et al. 2007). For this reason, size-dependent tree mortality under drought conditions is a matter of prime concern.

The wood density (WD) is often used as an indicative value for further xylem anatomical and hydraulic traits (Chave et al. 2009; Ziemińska et al. 2015), but studies find a varying degree of correlation between WD and xylem anatomy. While WD is closely related to vessel size and conductivity in semi-dry habitats with a pronounced dry season (Hoeber et al. 2014; Preston et al. 2006; Hietz et al. 2016), it often fails to predict xylem structure in perhumid tropical environments (Schuldt et al. 2013; Fortunel et al. 2014; Kotowska et al. 2015a; Poorter et al. 2010). Apparently, WD is mainly driven by the morphology of the tissue that makes up the largest cross-sectional area, usually fibres (Ziemińska et al. 2013; Zanne et al. 2010). Nevertheless, previous studies identified tropical trees with high WD to tolerate more negative water potentials (Santiago et al. 2004; Hacke et al. 2001), while those with light wood bear a greater risk of drought-induced die-back (Hietz et al. 2016; Poorter et al. 2010; Phillips et al. 2010) and this easily measurable trait might be an interesting predictor for xylem vulnerability, if the causal relationship can be deciphered (Meir et al. 2015).

Besides climatic stress, tropical rainforests suffer huge damage through anthropogenic land use. Forest clearing for timber, palm oil plantations and various other reasons have had a huge impact on this ecosystem over the past decades (Groombridge and Jenkins 2002; Giam 2017). A current hot-spot of these processes can be found on the Indonesian Island of Sumatra: Since the 1980s, large quantities of its tropical landscape got transformed into rubber and oil palm plantations (Miettinen et al. 2012; Margono et al. 2012). Additionally, a higher vulnerability to drought has been reported for southeast Asian rainforest, compared to Amazonian trees (Phillips et al. 2010) and the exceptional drought of 2015 led to an extensive removal of forest area due to the uncontrolled spreading of forest fires (Huijnen et al. 2016). This is why the island represents an especially interesting site to study the future development of tropical rainforests.

### 1.3 Aims and hypotheses

The objective of this thesis is to improve the understanding of drought resistance patterns in tropical tree species. Tree height, wood density and vessel anatomical features are thought to be key functional traits influencing growth and survival under drought conditions. Therefore, our aim is to explore the hydraulic diversity and xylem anatomy of eight Sumatran rainforest tree species and to find links between those traits and xylem vulnerability.

The following questions shall be investigated:

- (1) How do wood density and tree height at maturity relate to xylem vulnerability? We expect, that wood density and tree height influence xylem anatomy and xylem vulnerability. We hypothesize, that xylem safety will increase with higher wood density and decrease with tree height.
- (2) How do vessel anatomical traits differ between the investigated species? Do they influence xylem vulnerability? We hypothesize, that xylem safety decreases with vessel diameter and potential conductivity. We further expect a negative relationship between vessel diameter and vessel density.
- (3) How do the investigated species differ in their above ground biomass and growth rates? Does this have an influence on their xylem anatomy or safety? We expect, that tall trees have higher growth rates and potential conductivity and a lower xylem safety.

## 2. Methods

### 2.1 Study area and investigated species

The sampling was conducted in the Harapan rainforest in the province of Jambi (Sumatra, Indonesia). The area comprises about 100 000 ha of forest with a tropical humid climate. The annual mean temperature is 26.7 °C and the annual precipitation adds up to 2235 mm with a monthly rainfall of above 100 mm throughout the year (for more detailed information see Drescher et al. 2016).

The species selected for investigation represent a gradient of wood density and tree height at maturity (Table 1) and cover seven different plant families. The average tree height and wood density of the sampled individuals was checked to lay within the standard deviation frame of the average of all individuals on the research plots. Thus, it can be assumed, that no bias is introduced through the choice of sampled individuals.

### 2.2 Sample collection

We collected sun-exposed branches of mature trees, that did not show any sign of disease and represented the average habitus of each species. As these branches were in heights of 10 to 30 m, we used a *Notch BIG SHOT* launcher (SherrillTree; Greensboro, North Carolina, USA) to obtain samples, as described by Youngentob et al. (2016). With the slingshot, a weight bag with an attached rope was shot above the target branch. Subsequently, a chainsaw was attached to the rope and pulled on the branch, which was then sawn manually.

### 2.3 Maximum vessel length

The maximum vessel length (MVL, cm) of each species was estimated based on the air-injection method (Ewers and Fisher 1989; Cohen et al. 2003). Freshly sampled branches of about 1 to 2 m length were adapted with their distal end to a 50 ml syringe with attached barometer via *Tygon tubing* (Saint-Gobain Corporation; Courbevoie, France). With the syringe, we applied a pressure of 100 kPa, while the proximal end of the branch was immersed in water. Then, we consecutively cut segments of ca. 2 cm length, until a flow of air bubbles exiting the xylem was visible. At a pressure of 100 kPa, air cannot pass the intervessel pits and thus, no air bubbles appear at the open end as long as the vessel is still intact (Skene and Balodis 1968). As soon as air bubbles appeared at the cut end, the length of the remaining branch was measured and assumed to be equal to MVL of the individual. Between two and three MVL measurements were done per individual ( $n = 10 - 15$  values per species). For correlations with xylem vulnerability, we used the absolute maximum value.

Table 1: Characteristics of the eight investigated species. Average tree height of all sampled individuals (H, mean  $\pm$  SD) and the height of the tallest individual on the permanent sample plots, which is taken as the maximum tree height ( $H_{\max}$ ) under given growing conditions (Poorter et al. 2010). Wood density (WD, mean  $\pm$  SD), maximum vessel length (MVL, absolute maximum per species) and diameter at breast height (DBH, mean  $\pm$  SD). The number (n) of sampled tree individuals varied for xylem vulnerability measurements and anatomical analysis (in brackets).

Family	Species	Code	$n_{\text{sample}}$	H (m)	$H_{\max}$ (m)	WD (g cm <sup>-3</sup> )	MVL (cm)	DBH (cm)
Phyllanthaceae	<i>Aporosa nervosa</i>	Aner	5	17.4 $\pm$ 2.7	21.7	0.63 $\pm$ 0.05	57.8	17.1 $\pm$ 3.8
Rhizophoraceae	<i>Gynotroches axillaris</i>	Gaxi	5	21 $\pm$ 4.3	29	0.51 $\pm$ 0.07	75	23.8 $\pm$ 9.4
Fabaceae	<i>Koompassia malaccensis</i>	Kmal	4 (3)	34.8 $\pm$ 10.4	52.2	0.84 $\pm$ 0.03	23	45 $\pm$ 24.8
Euphorbiaceae	<i>Neoscortechinia kingii</i>	Nkin	5	16.6 $\pm$ 3.4	20.1	0.73 $\pm$ 0.03	10.8	14.7 $\pm$ 4.1
Melastomataceae	<i>Pternandra caerulescens</i>	Pcae	5	19.2 $\pm$ 4.9	29.6	0.59 $\pm$ 0.04	60.8	24.5 $\pm$ 12.5
Burseraceae	<i>Santiria apiculata</i>	Sapi	5 (4)	23.2 $\pm$ 8.7	35.6	0.6 $\pm$ 0.05	55.2	31.3 $\pm$ 19.3
Dipterocarpaceae	<i>Shorea ovalis</i>	Sova	5 (3)	28.6 $\pm$ 9.1	41.2	0.44 $\pm$ 0.06	97	41 $\pm$ 17.9
Dipterocarpaceae	<i>Shorea parvifolia</i>	Spar	5 (4)	25.8 $\pm$ 10.8	41.2	0.42 $\pm$ 0.09	66.6	31.8 $\pm$ 19.1

## 2.4 Xylem vulnerability to cavitation

In order to quantify the species vulnerability to cavitation, we used the bench dehydration method (Sperry et al. 1988; Choat et al. 2015). This method simulates drought conditions by bench-drying leafy branches for an extensive period of time, leading to the formation of embolisms inside the xylem (Sperry and Tyree 1988).

In the field, samples for bench dehydration were wrapped in opaque plastic bags, with the cut proximal ends in water to minimize dehydration. After 12 to 48 hours they were transported to the laboratory, where they were stored in water in a fridge at 4°C until the start of further processing. For every species, we tested 4 to 5 individuals (Table 1) and from each individual, 5 branches were collected and measured at different stages of dehydration, thus yielding 20 to 25 measurements per species. We used the 1.7-fold mean MVL of each species to determine the distance between the proximal cut end and targeted sample for conductance measurement in order to avoid air-entry artefacts that can bias the further measurements (Wheeler et al 2013; Torres-Ruiz et al. 2015). The dehydration was carried out under room conditions and cut surfaces were sealed with *Parafilm* (Bemis Company; Neenah, Wisconsin, USA) to prevent artificial evaporation. For each species, we tested drying times of 0.5 to 24 h. After the dehydration process, each branch was placed in an opaque plastic bag for 1 h, together with a moist towel, so that the water potential could equilibrate along the branch. However, we covered the leaves for the water potential measurement with aluminum foil and an extra plastic bag to avoid resaturation due to the humidified air in the equilibration-bag.

After equilibration, we measured the water potential of the leaves ( $\Psi$ , MPa) with a pressure chamber (*1505D-EXP*, PMS Instruments Company; Albany, Oregon, USA) as described by Scholander et al. (1964).  $\Psi$  of two leaves distal to the segment for conductance measurement per branch was measured by applying a slowly increasing air pressure on the leaf in the chamber, until the sap appears on the cut surface of the leaf petiole or rachis. The mean  $\Psi$  of these two measurements was used to build vulnerability curves. After measuring the water potential, each branch was prepared for conductance measurements with the *Xylem-Plus* embolism meter (Bronkhorst France; Montigny les Cormeilles, France). The branches were treated carefully to avoid removal of embolisms or induction of artefacts by cutting under tension (Torres-Ruiz et al. 2015). A 5 – 7 cm long subsegment was cut from the dehydrated branch under water to perform the conductance measurements. The segment was then connected with the proximal end to the *Xylem-Plus* and its initial conductance value (i.e. with embolized vessels,  $K_{init}$ ) was measured with a degassed solution at low pressure (ca. 6 kPa). We used a solution of deionized water to which 10 mM KCL and 1 mM CaCL<sub>2</sub> was added in order to recreate ionic concentration of natural sap (Zwieniecki et al. 2001; Nardini et al. 2012).

We also degassed the solution for at least 6 hours using a vacuum pump with an ultimate vacuum of 100 mbar (*ME1* diaphragm pump, Vacuubrand GMBH + CO KG; Wertheim, Germany). Afterwards, the same sample was flushed with the solution at high pressure (120 kPa) to remove embolisms. The conductance of the segment was then measured at low pressure 1 to 2 times until it reached its maximum value, considered to be the maximum conductance of the segment (i.e. without embolized vessels,  $K_{max}$ ; Choat et al. 2015).

To build xylem vulnerability curves, we plotted the percent loss of hydraulic conductivity (PLC, %) against  $\Psi$ , which is expected to be equal to xylem water potential due to the equilibration. PLC was calculated following the equation (1) of Choat et al. (2015).

$$PLC = \frac{100 \times (K_{max} - K_{init})}{K_{max}} \quad (1)$$

Vulnerability curves were calculated with the Weibull function and model equations were re-parameterized with  $P_{50}$  and slope at  $P_{50}$  (Ogle et al. 2009) to build equation (2), where  $P_{50}$  is the xylem pressure ( $\Psi$ ) at which 50 % of maximum conductivity ( $K_{max}$ ) is lost.

$$PLC = 100 \times \left( 0.5^{\left( \frac{\Psi}{P_{50}} \right)^{\left( \frac{-P_{50} \times slope}{50 \times \ln(0.5)} \right)}} \right) \quad (2)$$

## 2.5 Xylem anatomy and potential conductivity

We conducted the sampling along with sample collection for bench dehydration. For each tree individual, a branch subsection of 2 to 3 cm length and about 1 cm diameter was cut and stored in ethanol 70%. In the laboratory, the samples were cut into transverse sections of about 1 mm thickness, using a sliding microtome (*GSL 1*, Gärtner et al. 2014). The samples were then dyed with 1% safranin in 50% ethanol (Merck; Darmstadt, Germany) and washed with 70% ethanol. Afterwards, they were mounted on microscope slides, covered with euparal (Roth; Karlsruhe, Germany) and dried in an oven at 50°C for 10 to 20 days.

For anatomy investigation, we photographed each slide using a stereomicroscope (*SteREO Discovery.V20*, Zeiss; Jena, Germany). The Images were processed with the software *Adobe Photoshop CS6* (version c.13.0.1, Adobe Systems; San José, California, USA) and *ImageJ* (version 1.8.0\_112, open source). In *ImageJ* the measure [M] function was used to determine the total xylem area ( $A_{xylem}$ , mm<sup>2</sup>) and the particle analysis function yielded major and minor vessel diameter, as well as the total vessel number. With these values, we calculated the

vessel density (VD, n mm<sup>-2</sup>), total lumen area ( $A_{\text{lumen}}$ , mm<sup>2</sup>) and relative vessel lumen area ( $A_{\text{lumen}} : A_{\text{xylem}}$ , %).

For the estimation of vessel diameter ( $D$ ,  $\mu\text{m}$ ), the equation (2) of White (1991) was used. Parameters  $a$  and  $b$  represent major and minor vessel diameter, respectively.

$$D = \left( \frac{32 (ab)^3}{a^2 + b^2} \right)^{\frac{1}{4}} \quad (2)$$

Furthermore, the hydraulically weighted mean diameter ( $D_h$ ;  $\mu\text{m}$ ) was calculated, using the equation (3) given by Sperry et al. (1994).

$$D_h = \frac{\sum D^5}{\sum D^4} \quad (3)$$

The theoretical potential conductivity ( $K_p$ ; kg m<sup>-1</sup> MPa<sup>-1</sup> s<sup>-1</sup>) describes the maximal flow through the given size and number of vessels in each branch section. Thus, it is higher than the true conductivity, because the resistance of the vessel perforation plates, pit apertures (Sperry et al. 2005) and cavitated vessels are not considered. Nevertheless, it can be assumed, that the true conductivity scales positively with  $K_p$  (Poorter et al. 2010). It was calculated according to the Hagen–Poiseuille equation (4), where  $\eta$  is the viscosity of water (1.002 10<sup>-9</sup> MPa s) and  $\rho$  the density of water (998.2 kg m<sup>-3</sup>), both at 20°C.

$$K_p = \frac{\pi \sum D^4}{128\eta * A_{\text{xylem}}} \rho \quad (4)$$

## 2.6 Stand characteristics

The tree height ( $H$ , m) was recorded by Kotowska et al. (2015b) in August and September 2012. The total height was measured with a *Vertex III* height meter (Haglöf; Längsele, Sweden). If multiple measurements were taken, the maximum value was used.

The wood density (WD, g cm<sup>-3</sup>) was estimated in 2017, using a minimally invasive method (Parolin and Worbes 2000): Stem wood cores of ca. 50 – 80 mm length were sampled with an increment borer at 1.3 m height. WD was calculated as the ratio between the oven-dried mass of the core and its fresh volume (the cores were maintained in constant humidity). The volume was calculated from geometrical dimension (diameter and length measured with a caliper) assuming a perfect cylinder and the dry mass measured with a digital balance (precision at 0.001 g) after 72 h oven-drying at 70 °C.

The diameter at breast height (DBH, cm) was measured at 1.3 m height with a measuring tape (Richter Measuring Tools; Speichersdorf, Germany) in July 2016. For trees with buttresses or stilt roots, diameter was measured above stem anomalies. Stem growth increment was monitored with regular dendrometer tape (UMS; München, Germany) and documented every 2 – 4 months since 2013, for some individuals since 2016.

## 2.7 Data analysis

Statistical analyses were conducted in R (version 3.5.0, R Core Team 2018). For data handling and figure improvement the following packages were used: 'tidyverse' (Hadley Wickham 2017), 'tidyr' (Wickham and Henry 2018), 'magrittr' (Bache and Wickham 2014), 'lubridate' (Grolemund and Hadley Wickham 2011), 'psych' (Revelle 2018), 'broom' (Robinson and Hayes 2018), 'scales' (Hadley Wickham 2018), 'gridExtra' (Auguie 2017), 'ggpubr' (Kassambara 2018) and 'ggthemes' (Arnold 2018). Statistical tests were regarded as significant at  $p \leq 0.05$ .

We checked the normal distribution of data visually with histograms and we log-transformed some variables ( $D$ ,  $D_h$ ,  $VD$ ,  $K_p$  and  $A_{\text{lumen}} : A_{\text{xylem}}$ ) to obtain gaussian distributions. Subsequently, an analysis of variance (ANOVA) was performed for every potential predictor for xylem vulnerability to test for significant differences between species. To further elucidate the statistical differences among single species, we conducted a post-hoc test (Turkey's Test) and extracted the indicative letters with the 'multcomp' package (Hothorn et al. 2008).

Interrelationships between the investigated traits, as well as correlations with xylem vulnerability, were tested with a Pearson correlation analysis, by plotting one trait against another and running a linear regression analysis. Correlation matrices were obtained using the 'Hmisc' package (Harrel 2018).

We computed the aboveground biomass (AGB, kg) with the 'BIOMASS' package (Rejou-Mechain et al. 2018). Tree height, wood density and stem diameter were included in the calculation.

### 3. Results

#### 3.1 Tree structural traits and growth

Two statistically different groups can be found within the investigated species in regard to their height (Figure 3A). *A. nervosa* and *N. kingii* are the smallest trees, while *K. malaccensis* is significantly taller. The other five species *G. axillaris*, *P. caerulescens*, *S. apiculata*, *S. ovalis* and *S. parvifolia* are medium sized and do not differ significantly from the other two groups. As a top canopy species, *K. malaccensis* can reach heights of above 50m (Table 1). The medium sized species range from about 20 to 30 m at average height and the smallest group shows an average height of below 20 m.

Regarding wood density, most species can be divided into three distinct statistical groups (Figure 3B). *K. malaccensis* is again an outstanding species with the highest average value for wood density ( $0.84\text{ g cm}^{-3}$ , Table 1). The lowest wood density can be found in the two *Shorea* species ( $0.44$  and  $0.42\text{ g cm}^{-3}$ ). *P. caerulescens* and *S. apiculata* are in between with wood densities of  $0.59$  and  $0.6\text{ g cm}^{-3}$ . The other 3 species are intermediate and do not differ significantly from these three groups.

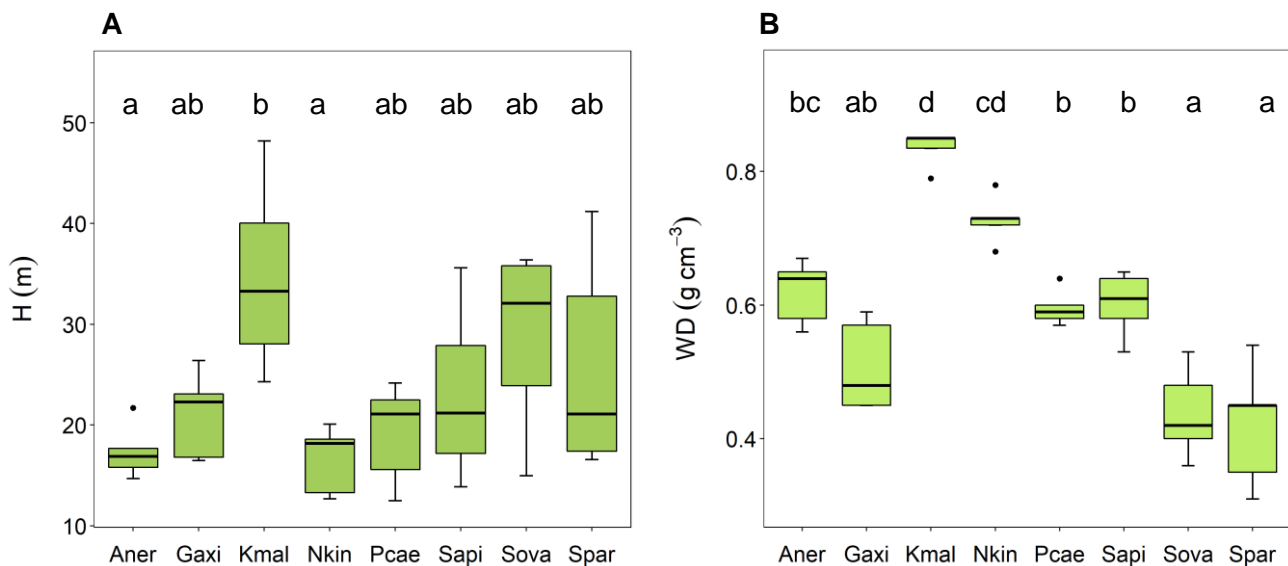


Figure 3: Tree structural traits. Boxplot of tree height (H) and wood density (WD) of the investigated species. Only sampled individuals are considered (for more detailed information see Table 1). Letters indicate significant differences (ANOVA  $p \leq 0.05$ , Tukey),  $n = 5$  per species (*K. malaccensis*:  $n = 4$ ).

AGB of the investigated trees differed greatly, ranging from less than 100 kg to more than 10.000 kg for single individuals (Figure 4). All species show a large intraspecific variance of AGB values, which is in line with the varying tree heights within each species. Therefore, an ANOVA did not yield significantly different groups, except for *K. malaccensis* and *N. kingii* which differ significantly in their AGB (Appendix 1).

As a tall species with additional high wood density, *K. malaccensis* is among the most massive trees. The two *Shorea* species as well as *S. apiculata* reach AGB values of 1000 kg and more, while the other species do exceed mass of 1000 kg. All individuals of *A. nervosa* and *N. kingii* are less than 400 kg. *G. axillaris* and *P. caerulescens* are intermediate with a broad range from less than 100 kg to more than 900 kg.

The annual growth rates reach top values of more than 7 % for some individuals, but most trees showed annual growth rates of about 2 – 3% (Appendix 1).

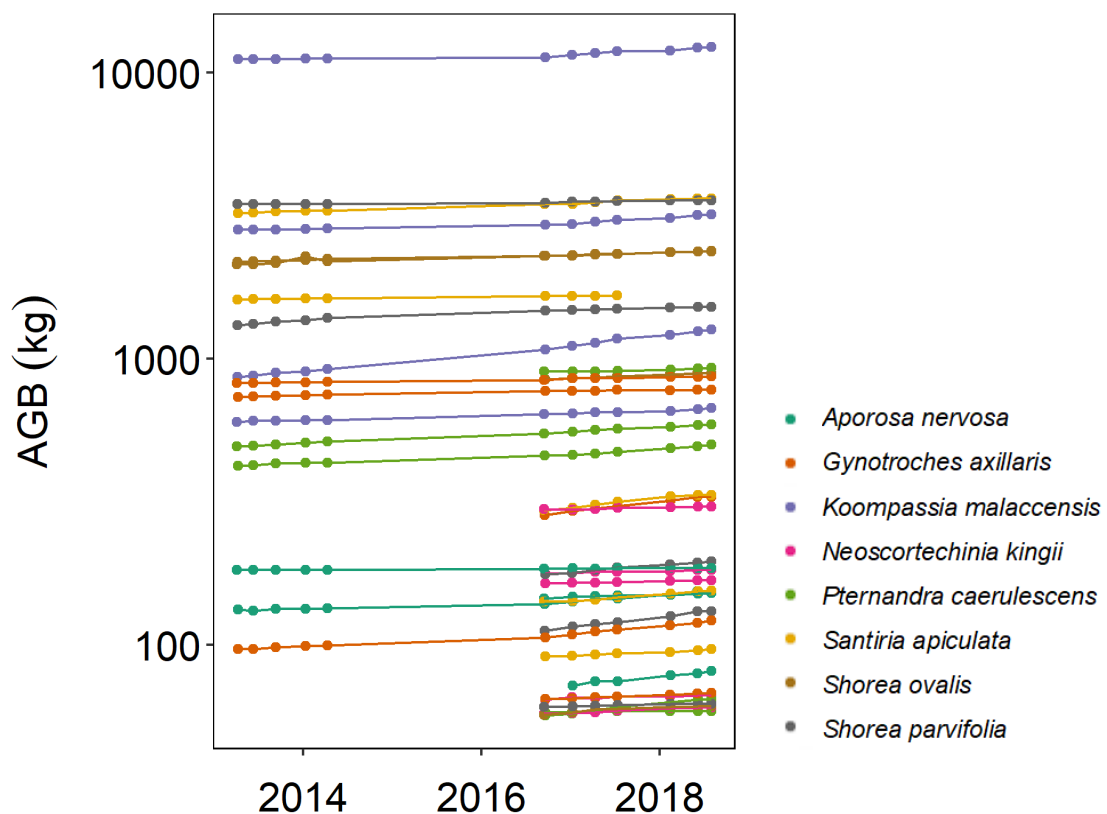


Figure 4: Development of the aboveground biomass (AGB) from year 2013 to 2018. All sampled individuals are considered (n = 39).

### 3.2 Xylem anatomy

The investigated species show a high variability in xylem anatomical traits. Variation in median values between species ranged from 1.5-fold ( $D_h$ ) to more than 6-fold in MVL (Figure 5 and Appendix 2), but the high intraspecific variance within some species also caused an extensive overlapping and hence many species were statistically indistinctive from each other. For most investigated traits, we see a pattern with one or two distinct species at each end of the spectrum, while the other species are intermediate without significant differences among them.

The largest  $D$  can be found in *K. malaccensis* with a median of about 55  $\mu\text{m}$  (Figure 5A). This species is statistically similar to other large vessel species like *S. ovalis*, *S. parvifolia* and *G. axillaris*. The smallest vessels were identified in *S. apiculata* as well as *N. kingii* and *P. caerulescens*. Only *A. nervosa* differs significantly from both *K. malaccensis* and *S. apiculata* and thus has medium sized vessels.  $D_h$  shows a similar distribution to the mean vessel diameter, with *K. malaccensis* and the *Shorea* species having the highest values (Figure 5B), while *S. apiculata* has the smallest conducting vessel diameter. Vessel densities (VD) follow an opposite trend to vessel diameters: The highest densities are found in *S. apiculata* and the lowest in *K. malaccensis* with medians of about 100 and 35 vessels per  $\text{mm}^2$  (Figure 5C). All other species do not differ significantly from each other, with medians ranging from 50 to 70 vessels per  $\text{mm}^2$ , except for *Shorea ovalis* which has a median of about 85 vessels per  $\text{mm}^2$ , despite its large average vessel diameter. This makes *S. ovalis* an exception from the general trend, that those species with a large average vessel diameter have lower vessel densities.

$K_p$  (Figure 5D) is highest in the two *Shorea* species and *K. malaccensis* with medians of more than  $15 \text{ kg m}^{-1} \text{ MPa}^{-1} \text{ s}^{-1}$ , while all other species have a median of about  $10 \text{ kg m}^{-1} \text{ MPa}^{-1} \text{ s}^{-1}$  or lower. However, the differentiation between species is statistically not clear. For MVL, the post-hoc test yielded two distinct groups: *N. kingii* shows by far the shortest maximum vessel lengths (median of about 10cm, Figure 5E), while *G. axillaris*, *P. caerulescens* and the two *Shorea* species have significantly longer maximum vessel lengths. The other three species are intermediate and thus not significantly different from both groups. The relative vessel lumen area ( $A_{\text{lumen}} : A_{\text{xylem}}$ ) of each species is pictured in Figure 5F. *Shorea ovalis* has the highest lumen percentage with more than 20%. *S. parvifolia* and *A. nervosa* also show large proportions of vessel lumen and are thus not significantly different. *N. kingii* has the lowest fraction of vessel lumen and is significantly differing from the beforementioned species, but similar to the other four species *G. axillaris*, *K. malaccensis*, *P. caerulescens* and *S. apiculata*.

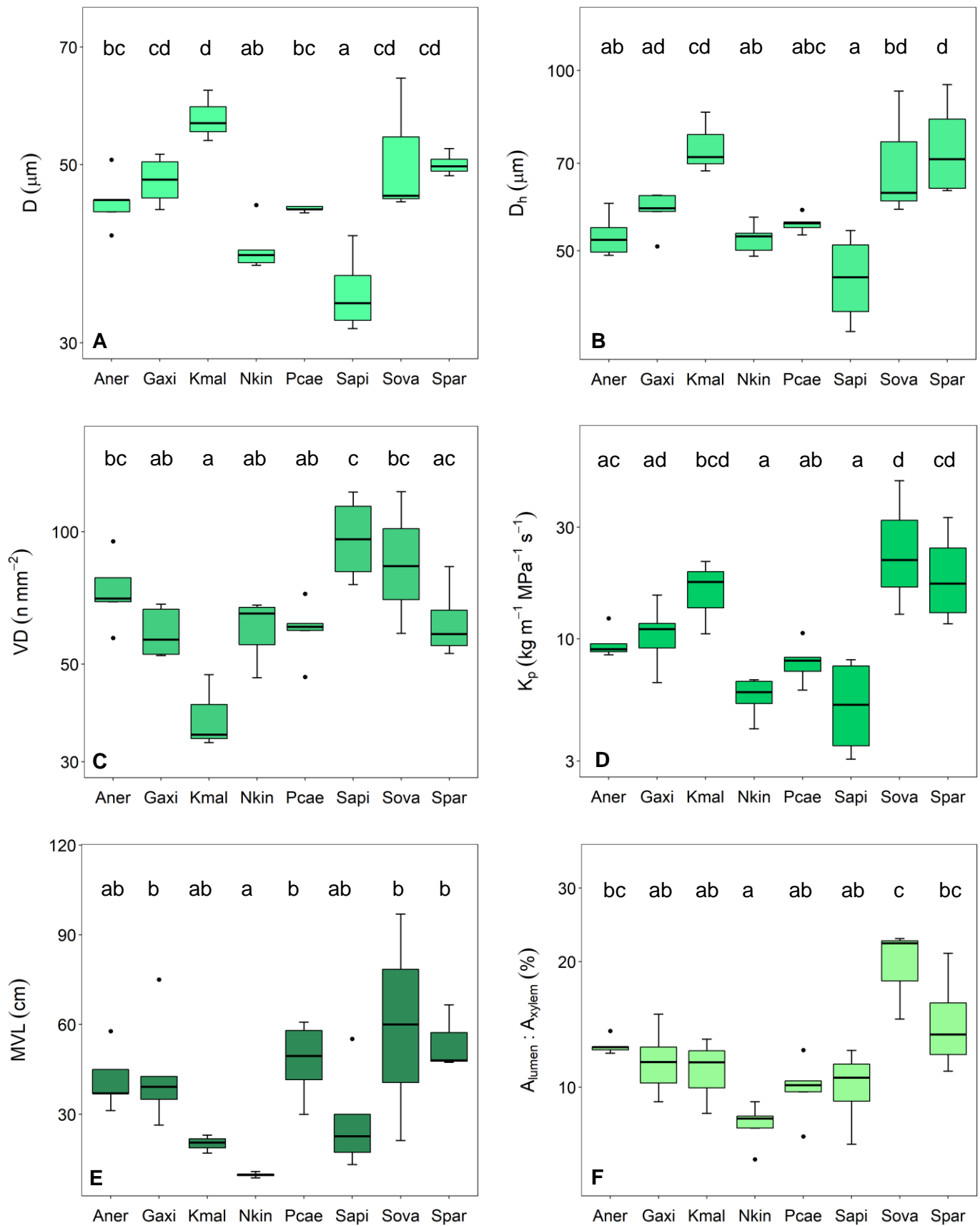


Figure 5: Xylem anatomy. Box plots of the analyzed xylem anatomical traits in the eight investigated species. Letters indicate significant differences of means ( $p \leq 0.05$ , Tukey). A: Mean vessel diameter ( $D$ ). B: Mean hydraulic vessel diameter ( $D_h$ ). C: Vessel density ( $VD$ ). D: Potential hydraulic conductivity ( $K_p$ ). E: Maximum vessel length ( $MVL$ ). F: Relative vessel lumen area ( $A_{\text{lumen}} : A_{\text{xylem}}$ ).

### 3.3 Vulnerability curves

The key results of this study are the xylem vulnerability curves for the eight investigated tree species (Figure 6). The significance for all  $P_{50}$  values is high ( $p \leq 0.001$  for most species,  $p = 0.002$  for *A. nervosa*), while the calculated slope value is not significant for *A. nervosa* and *K. malaccensis* (for detailed  $p$  values and  $t$  statistic see Appendix 7).

$P_{50}$  values vary about 1.5 MPa between the most vulnerable and the most resistant species. The highest  $P_{50}$  and thus the lowest xylem resistance is found in *S. apiculata* (-1.3 MPa), which is followed by *G. axillaris* (-1.51 MPa). The two *Shorea* species and *A. nervosa* have a mediate  $P_{50}$  compared to the other species, ranging from -1.62 to -1.72 MPa. The lowest  $P_{50}$  and therefore the highest xylem resistance can be accounted to *K. malaccensis*, *P. caerulescens* and *N. kingii* with  $P_{50}$  values below -2 MPa (-2.25, -2.59 and -2.76 MPa respectively).

The slopes at  $P_{50}$  are variable among species as well. A high slope value indicates a fast progress in embolization under drought conditions, while species with lower slope values experience a rather slow loss of their conductivity. The highest slope can be found in the most vulnerable species *S. apiculata* (50.1), which is followed by the most resistant species *N. kingii* (32.7) and by *S. parvifolia* (30.9). The slope values of all other species vary between 22 and 23.7. This observation suggests that there is no dependence of the overall xylem resistance ( $P_{50}$ ) with the progress of embolization. Indeed, a correlation analysis did not yield a significant relationship between these two variables (Table 2).

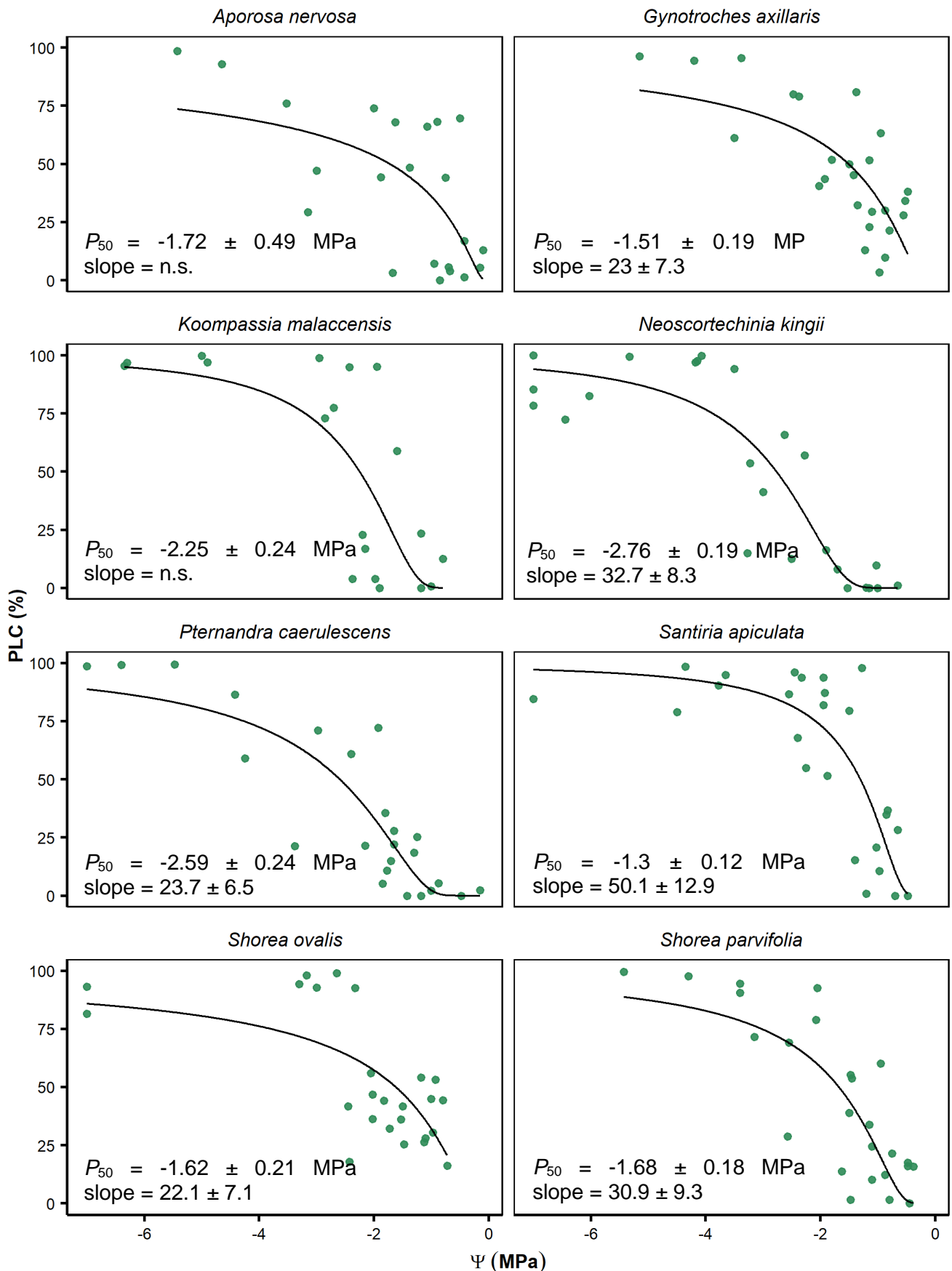


Figure 6: Vulnerability curves. Percentage loss of hydraulic conductivity (PLC) versus leaf water potential ( $\Psi$ ) for the eight investigated tree species. Slope indicates the slope at 50% loss of conductivity ( $P_{50}$ ).  $p \leq 0.05$  for all indicated values, n.s. indicates that value is not significant.  $n = 25$  for every species, except for *K. malaccensis*, which has  $n = 20$ .

### 3.4 Associations among the investigated traits

Several xylem traits were correlated with wood density across all species. MVL and WD correlate negatively, indicating that longer vessels reduce wood density (Figure 7D), this relationship remains significant if MVL per species and mean WD per species are correlated with each other (Table 2). Wood density and D were found to be unrelated (Figure 7A), indicating that the mean vessel diameter has no influence on WD. The relative vessel lumen area however does correlate negatively with WD, as a lower lumen fraction is associated with higher WD (Figure 7B).  $K_p$  and WD are negatively related as well, thus a higher  $K_p$  leads to a decrease in wood density (Figure 7C). In addition,  $A_{\text{lumen}} : A_{\text{xylem}}$  is positively correlated with  $K_p$  across all species and also if mean values per species are tested (Table 2).

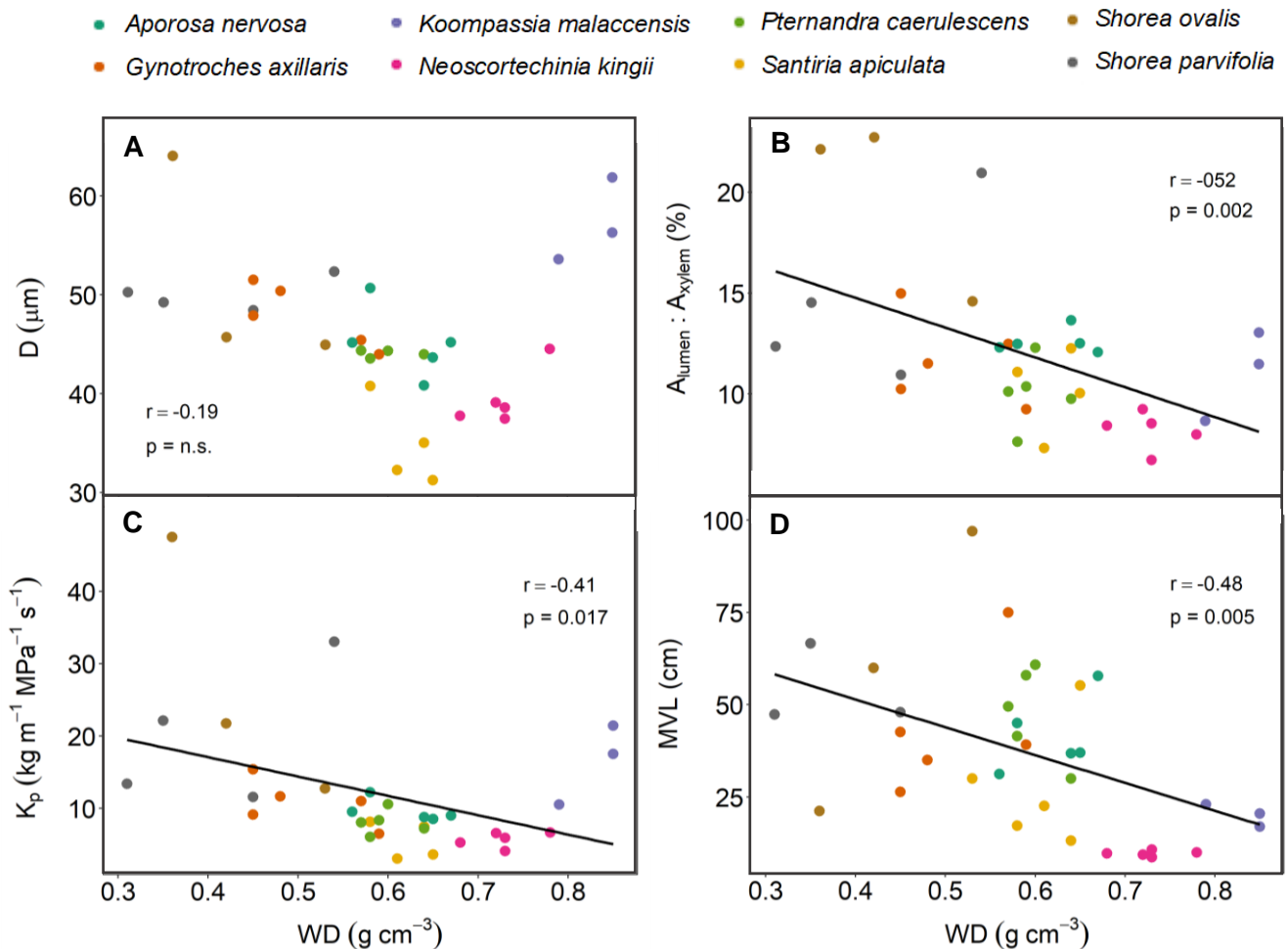


Figure 7: Wood density (WD) in relation to xylem anatomical traits across all species ( $n = 34$ ). A: Mean vessel diameter (D). B: Relative vessel lumen ( $A_{\text{lumen}} : A_{\text{xylem}}$ ). C: Potential conductivity ( $K_p$ ). D: Maximum vessel length (MVL). n.s. indicates that value is not significant ( $p > 0.05$ ).

Tree height was found to correlate with only two vessel traits across all species, while conductivity, relative vessel area and wood density were unrelated with individual tree height.  $D_h$  is significantly correlated with  $H$  across all species (Figure 8, top) and also if mean values per species are correlated (Table 2). This correlation is positive, indicating, that tall trees develop wider vessels in their sun-exposed canopy branches. The mean  $D_h$  per species also scales positively with  $H_{max}$  (Table 2), which suggests that tall growing tree species have vessels with higher conductive diameter, independent of individual tree height. The maximum vessel diameter ( $D_{max}$ ), which is the widest vessel found in each individual, is positively correlated with tree height as well (Table 2). In contrast,  $D$  does not show a significant correlation with tree height across or within species (Figure 8, bottom). The overall trend is positive, but if correlated within species, *K. malaccensis*, *S. ovalis* and *G. axillaris* show a reduction in mean vessel diameter with tree height, while for *N. kingii* and *P. caerulea*, the height does not influence mean vessel diameters. However, the mean  $D$  and the mean  $H$  per species do show a significant positive relationship (Table 2).

None of the proposed determinants shows a significant correlation with the two investigated measures for xylem vulnerability  $P_{50}$  and slope at  $P_{50}$  (Table 2). Especially the mean vessel diameter, a trait that was expected to have a strong influence on xylem vulnerability, was found

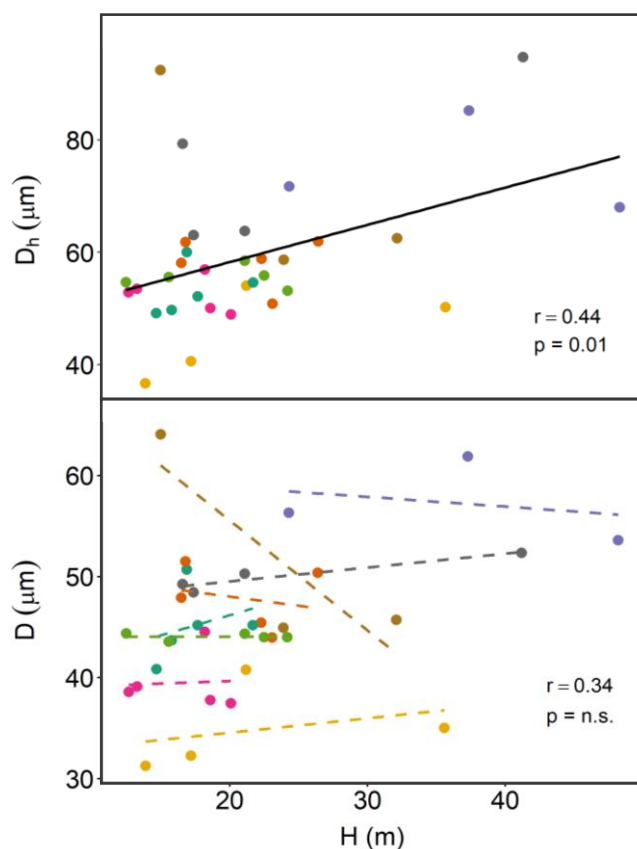


Figure 8: Tree height ( $H$ ) in relation to hydraulic vessel diameter ( $D_h$ , top) and mean vessel diameter ( $D$ , bottom). Species are colored according to the legend in Figure 7.

Full lines indicate significant relationships, while dotted lines indicate non-significant relationships for every single species ( $n = 3$  to  $5$ ).  $r$  and  $p$  value are the parameters of the overall relationship. n.s.: value is not significant ( $p > 0.05$ ).

to have a correlation coefficient close to zero (Figure 9D). Similarly, the potential conductivity shows no significant relationship with  $P_{50}$  and only a low coefficient of correlation (Figure 9C). Also, the wood density is not significantly correlated with the  $P_{50}$ , although the correlation coefficient indicates a negative trend, driven by low wood density species like *K. malaccensis* and *N. kingii*, which also display high xylem resistance (Figure 9A). Tree height was neither correlated to  $P_{50}$  (Figure 9B). This is also true for  $H_{max}$  (Table 2). However, MVL shows a high coefficient of correlation ( $r = 0.56$ ) with  $P_{50}$ , although the relationship is not significant.

VD and D show a negative correlation across all species, but if species means are tested, this relationship becomes insignificant, although the correlation coefficient remains almost the same ( $r = -0.55$  and  $r = -0.57$ , Table 2). Annual AGB growth rate of is not related to xylem vulnerability or any other of the investigated variables and does not vary significantly among most species (Appendix 1). Notably, its highest correlation value was found with  $P_{50}$  and slope (Table 2), even if the relation is not significant.

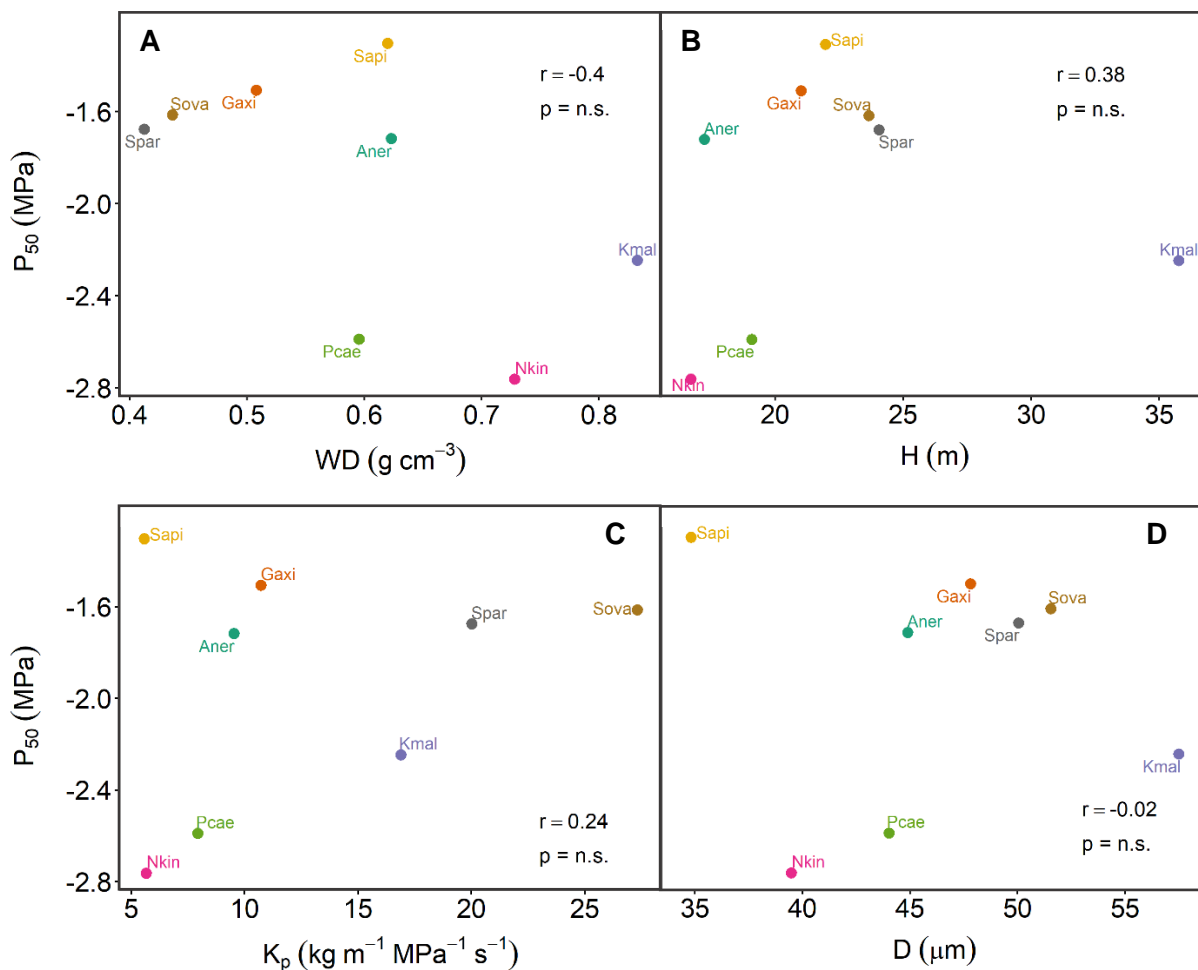


Figure 9:  $P_{50}$  in relation to its four expected main predictors: A: Wood density (WD), B: Tree height (H), C: Potential conductivity ( $K_p$ ) and D: Mean vessel diameter (D). Species codes according to Table 1. n.s. indicates that the value is not significant ( $p > 0.05$ ).

Table 2: Pearson correlation for Xylem vulnerability and 11 relevant tree structural and xylem anatomical traits. Upper half: Correlation across the eight investigated tree species, n = 34. Lower half: Correlation on species level (mean or maximum values per species, n = 8).

	$P_{50}$	Slope	$H_{max}$	H	WD	D	$D_h$	$D_{max}$	VD	$K_p$	MVL	$A_{lumen}$ : $A_{xylem}$	Growth AGB (%)
<b>Slope</b>	r = 0.08 p = 0.855												
$H_{max}$	r = 0.22 p = 0.595	r = 0.42 p = 0.304											
H	r = 0.07 p = 0.871	r = 0.41 p = 0.314	<b>r = 0.93</b> <b>p = 0.001</b>		r = 0.2 p = 0.245	r = 0.34 p = 0.052	<b>r = 0.44</b> <b>p = 0.01</b>	<b>r = 0.47</b> <b>p = 0.005</b>	r = -0.04 p = 0.831	r = 0.26 p = 0.133	r = -0.06 p = 0.721	r = 0.24 p = 0.163	r = -0.31 p = 0.079
WD	r = -0.56 p = 0.149	r = 0.37 p = 0.365	r = 0.01 p = 0.975	r = 0.31 p = 0.451		r = -0.19 p = 0.278	r = -0.24 p = 0.174	r = -0.22 p = 0.208	r = -0.18 p = 0.298	<b>r = -0.41</b> <b>p = 0.017</b>	<b>r = -0.48</b> <b>p = 0.005</b>	<b>r = -0.52</b> <b>p = 0.002</b>	r = -0.31 p = 0.072
D	r = -0.02 p = 0.958	r = -0.3 p = 0.476	r = 0.67 p = 0.067	<b>r = 0.73</b> <b>p = 0.041</b>	r = -0.03 p = 0.941		<b>r = 0.87</b> <b>p &lt; 0.001</b>	<b>r = 0.59</b> <b>p &lt; 0.001</b>	<b>r = -0.55</b> <b>p = 0.001</b>	<b>r = 0.77</b> <b>p &lt; 0.001</b>	r = 0.06 p = 0.72	<b>r = 0.51</b> <b>p = 0.002</b>	r = -0.08 p = 0.641
$D_h$	r = 0.01 p = 0.98	r = -0.11 p = 0.794	<b>r = 0.76</b> <b>p = 0.028</b>	<b>r = 0.72</b> <b>p = 0.046</b>	r = -0.2 p = 0.635	<b>r = 0.91</b> <b>p = 0.002</b>		<b>r = 0.86</b> <b>p &lt; 0.001</b>	<b>r = -0.36</b> <b>p = 0.038</b>	<b>r = 0.9</b> <b>p &lt; 0.001</b>	r = 0.03 p = 0.854	<b>r = 0.64</b> <b>p &lt; 0.001</b>	r = -0.03 p = 0.885
$D_{max}$	r = 0.24 p = 0.563	r = 0.02 p = 0.966	r = 0.54 p = 0.171	r = 0.36 p = 0.381	r = -0.54 p = 0.168	r = 0.5 p = 0.206	<b>r = 0.77</b> <b>p = 0.026</b>		r = -0.13 p = 0.468	<b>r = 0.77</b> <b>p &lt; 0.001</b>	r = 0.04 p = 0.834	<b>r = 0.62</b> <b>p &lt; 0.001</b>	r = -0.07 p = 0.684
VD	r = 0.61 p = 0.105	r = 0.12 p = 0.782	r = -0.19 p = 0.656	r = -0.43 p = 0.291	r = -0.47 p = 0.244	r = -0.57 p = 0.138	r = -0.44 p = 0.272	r = -0.13 p = 0.762		r = -0.05 p = 0.765	r = 0.27 p = 0.134	<b>r = 0.38</b> <b>p = 0.027</b>	r = 0.19 p = 0.289
$K_p$	r = 0.28 p = 0.501	r = -0.23 p = 0.584	r = 0.66 p = 0.073	r = 0.5 p = 0.205	r = -0.48 p = 0.232	<b>r = 0.76</b> <b>p = 0.029</b>	<b>r = 0.87</b> <b>p = 0.005</b>	r = 0.68 p = 0.064	r = 0.02 p = 0.969		r = 0.11 p = 0.558	<b>r = 0.84</b> <b>p &lt; 0.001</b>	r = 0.04 p = 0.82
MVL	r = 0.66 p = 0.073	r = -0.43 p = 0.289	r = 0.12 p = 0.77	r = -0.14 p = 0.737	<b>r = -0.87</b> <b>p = 0.005</b>	r = 0.16 p = 0.707	r = 0.18 p = 0.671	r = 0.28 p = 0.499	r = 0.52 p = 0.182	r = 0.53 p = 0.174		<b>r = 0.37</b> <b>p = 0.033</b>	r = 0.3 p = 0.087
$A_{lumen}$ : $A_{xylem}$	r = 0.5 p = 0.203	r = -0.37 p = 0.361	r = 0.42 p = 0.298	r = 0.2 p = 0.632	r = -0.68 p = 0.066	r = 0.52 p = 0.188	r = 0.6 p = 0.113	r = 0.53 p = 0.174	r = 0.36 p = 0.385	<b>r = 0.91</b> <b>p = 0.002</b>	<b>r = 0.77</b> <b>p = 0.025</b>		r = 0.09 p = 0.61
<b>Growth</b> AGB (%)	r = 0.42 p = 0.306	r = 0.44 p = 0.279	r = 0.36 p = 0.388	r = 0.27 p = 0.522	r = -0.21 p = 0.626	r = -0.05 p = 0.905	r = 0.03 p = 0.94	r = 0.34 p = 0.408	r = -0.03 p = 0.941	r = -0.15 p = 0.73	r = 0.16 p = 0.711	r = -0.19 p = 0.657	

## 4. Discussion

### 4.1 Predictors for xylem safety

The main aim of this study was to determine xylem vulnerability of the eight investigated species. The calculated  $P_{50}$  values vary more than twofold from -1.3 to -2.76 MPa between species, indicating that they have distinctive xylem drought resistances. In the literature,  $P_{50}$  of woody plants range from -0.25 to -14 MPa (Pérez-Harguindeguy et al. 2013). Thus, the species in this study can be considered as vulnerable to drought-induced embolism compared to species across all habitats, but compared to other species from regions with an annual rainfall of 2000 to 2500 mm they fall within the regular range (Choat et al. 2012).

Overall, *P. caerulescens*, a species which displays intermediate characteristics for most xylem anatomical traits (Figure 5), seems to be the most drought resistant species regarding its xylem system, because of its low  $P_{50}$  (-2.59 MPa) as well as low slope value (23.65). In contrast, *S. apiculata*, a small vessel species, appears to have the most vulnerable xylem towards water deficits, having the highest  $P_{50}$  (-1.3 MPa) and highest slope value (50.14).

A further aim of this study was to analyze xylem anatomy and hydraulic traits of the eight investigated species and to relate them with wood density and tree height. In our dataset, vessel diameter traits ( $D$ ,  $D_h$ ,  $D_{max}$ ) and VD are not correlated with wood density. This is in line with other studies from perhumid habitats without a dry season (Schuldt et al. 2013; Kotowska et al. 2015a; Fortunel et al. 2014; Poorter et al. 2010). We found a higher potential conductivity to be associated with light wood ( $r = -0.41$ ), but previous investigations produced mixed results regarding this relationship (Chave et al. 2009; Zanne et al. 2010) and recently it has been demonstrated that WD is mainly determined by fibre cell wall thickness (Ziemińska et al. 2013; 2015). Hence, the correlations with xylem anatomy and hydraulic traits found in our study can be assumed to be indirect. This is also the case for the observed relationships of WD with MVL and  $A_{lumen} : A_{xylem}$ . However, the significant relation of  $A_{lumen} : A_{xylem}$  and WD suggests, that that the non-vessel-lumen-fraction must have a similar density across all species, so that variations in  $A_{lumen} : A_{xylem}$  have a measurable influence.

High WD is often found to co-occur with more negative water potentials in natural conditions (Santiago et al. 2004; Preston et al. 2006) and lower mortality rates under drought conditions (Phillips et al. 2010; Hietz et al. 2016). This is thought to be related to the greater mechanical stability, which allows a higher tolerance towards negative water potentials (Hacke et al. 2001). In our dataset, species with medium WD vary widely in their xylem vulnerability (-2.59 to -1.3 MPa). Similarly, Ziemińska et al. (2015) observed that a wide range of wood structures produces medium wood densities. The species with the lowest WD (*S. ovalis* and *S. parvifolia*)

belong to the 50% most vulnerable species, while *K. malaccensis*, with the highest WD, is amongst the most resistant species. But overall, we could not find a significant relationship between WD and xylem safety. This is actually in line with the finding that WD is chiefly determined by fibre wall thickness (Ziemińska et al. 2013), which suggests that the association of WD and xylem vulnerability can be assumed to be indirect, just as the relation of vessel size and WD.

Tall trees are the most vulnerable group of rainforest trees under drought conditions, as their mortality rates are substantially elevated, compared to small trees (da Costa et al. 2010; Phillips et al. 2010; Zhang et al. 2009). This has been linked to hydraulic failure (Bennett et al. 2015; Rowland et al. 2015) and subsequently one can assume, that the hydraulic architecture and xylem anatomy of large trees differs from those in smaller trees. Indeed, in this study, the individual tree height and  $D_h$  as well as  $D_{max}$  are positively correlated across all species, which has been confirmed by others as well (Zach et al. 2010; Olson et al. 2014).

While the individual D and the individual H show no significant correlation, mean D and mean H per species are positively related (Table 2). This indicates that the D/H relationship is different among species, which is also visible in Figure 8B: Some species (*A. nervosa*, *S. apiculata* and *S. parvifolia*) develop wider vessels if they are higher, others narrower vessels (*K. malaccensis*, *S. ovalis* and *G. axillaris*). In *N. kingii* and *P. caerulescens* the mean vessel diameter is independent from individual height. This can be interpreted as a strategy-dependent feature. Tall mature-phase trees (*K. malaccensis*, *S. ovalis*) need to grow fast in juvenile stages in order to efficiently use canopy gaps and to reach reproductive maturity. In order to facilitate high growth rates, they need to develop wide vessels for an efficient water transport (Santiago et al. 2004). But once they grew to a sufficient height, they switch strategies and invest more in xylem safety. On the contrary, Pioneer species aim for maximum growth throughout their life span, continuing to increase vessel size with tree height. Understorey trees (*N. kingii*, *P. caerulescens*) maintain low growth rates and are not exposed to higher evaporation rates in the canopy layer, thus having small vessels, independent from tree height. In the literature, a positive relationship between conductivity and tree height is commonly described (Hietz et al. 2016; Apgaua et al. 2016; Poorter et al. 2010; Preston et al. 2006). Although, some studies report the opposite trend: Conductivity decreases with H, which was also associated with an increase of WD with H (Zhang et al. 2009). In our data set,  $K_p$  and H vary independently. This could be caused by contrasting trends within species, which follow the within-species correlations of D (data not shown) and that mask a clear across-species pattern.

In line with elevated drought-induced mortality rates in large trees, a positive correlation of  $P_{50}$  with tree height has been observed in previous studies (Rowland et al. 2015). The underlying

assumption, that tree height and vessel anatomy are correlated, could be confirmed by our data since tree height and  $D_h$  as well as  $D_{max}$  scale positively in our dataset. Nevertheless, this finding in xylem anatomy did not translate into significant height influence on xylem vulnerability ( $P_{50}$  or slope) across the investigated species in this study:

The  $P_{50}$  values of medium sized species with an average height of 20 to 30 m (*G. axillaris*, *P. caerulescens*, *S. apiculata*, *S. ovalis* and *S. parvifolia*) vary widely, from -1.51 to -2.59 MPa. The smallest species (*A. nervosa* and *N. kingii*) with an average height of below 20 m, display both very low (-1.72 MPa) and very high (-2.76 MPa) values and the tallest species *K. malaccensis* is, in contrast to our expectations, among the most resistant species (-2.25 MPa). This illustrates that the relationship between H and xylem vulnerability is inconsistent in our dataset, hence not allowing inferences on xylem safety through H.

In general, complex traits like WD and H appear not to be reliable predictors of xylem vulnerability. Often, combinations of traits are found within species and thus a causal relationship between them is inferred. An example is the co-occurring of high WD, small vessels, low vessel density, low conductivity, thick cell walls with thick and lowporous pit membranes in combination with high xylem safety (Hoeber et al. 2014; Li et al. 2016; Cosme et al. 2017), especially in dry or semi-dry habitats. All of those traits have been explained to directly influence xylem safety (see above) but contrasting results in different studies suggest the opposite. The main determinant of xylem safety has not been identified yet (Meir et al. 2015), and the results from this study suggest, that it is none of the herein assessed traits. Promising candidates are thickness and porosity of pit membranes (Li et al. 2016).

In contradiction to our expectations, neither the investigated xylem anatomical traits nor the xylem vulnerability measures ( $P_{50}$ , slope) showed a significant correlation with annual growth rates of aboveground biomass. The trait that is most commonly recognized to influence growth in tropical trees is wood density (Chave et al. 2009; Poorter et al. 2010; Hietz et al. 2016; Kunstler et al. 2016). This is explained by the lower costs of light wood tissue and often, this also comes along with a higher xylem conductivity (Kotowska et al. 2015a; Poorter et al. 2018), which in turn enables faster growth through an extensive water supply (Santiago et al. 2004). While WD and  $K_p$  are indeed related in our dataset (see above), none of these traits had a significant influence on the growth rates (Table 2). Additionally, the annual percentage of growth was very similar for all species and only *K. malaccensis* was statistically distinctive (Appendix 1). Poorter et al. (2018) point out, that environmental conditions can cause a strong convergence in growth rates in slow-growing tropical rainforests, which is a possible explanation for the similarity of our species. Furthermore, they suggest, that the increment in stem diameter might be a poor measure for tree growth, as trees could invest more into height or leaf growth to enhance light exploitation.

However, in all the abovementioned studies, growth rate was correlated with wood anatomical traits. So, it should be considered, that our data do not reflect the correct diameter increment, e.g. due to inaccurate reading of dendrometer values. In the course of the last years, dendrometer reading was done by different people, some of them were field assistants without biological or scientific background. Thus, imprecisions in diameter documentation could have biased our data.

An unexpected result was the high correlation coefficient between MVL and  $P_{50}$ , even if not significant. This could give evidence for the effective restriction of embolisms through frequent end walls and intervessel pits (Comstock and Sperry 2000).

#### **4.2 Efficiency/ safety trade-off**

As expected, we observed a highly significant negative correlation between D and VD across all species. This provides further evidence for the well-known trade-off between hydraulic efficiency and hydraulic safety (Sperry et al. 2008; Zanne et al. 2010; Poorter et al. 2010; van der Sande et al. 2019). However, *S. ovalis* was found to have wide vessels and a high vessel density with a high variability in both traits. This facilitates an exceptional high  $K_p$  in this species, but also causes relatively high xylem vulnerability (Figure 9C). We could not find a significant correlation between xylem vulnerability ( $P_{50}$ ) and efficiency ( $K_p$ ), but we also did not find a species with low  $P_{50}$  and high  $K_p$ —the right lower corner of Figure 9C is empty, whereas some species show a low conductivity and safety (*S. apiculata*, *A. nervosa* and *G. axillaris*). This phenomenon has already been observed by Gleason et al. (2016), who reported a weak correlation due to species with low efficiency and safety. Eventually the perhumid environment weakens the effect of the efficiency/ safety trade-off (Choat et al. 2012), as water deficits are rare.

Another potential reason for the disconnection of  $P_{50}$  and conductivity is that for this study, a theoretical conductivity was calculated, but no true conductivity was measured. Thus, the resistance of vessel perforation plates and intervessel pits is not considered (Sperry et al. 2005; Choat et al. 2008). Kotowska et al. (2015a) report, that the empirical conductivity is less than 50% of the theoretical one for most species, indicating that the differences are substantial. The adaptive pressure works on the true conductivity, not on the theoretical one. For future analysis it would be interesting to correlate true conductivity with  $P_{50}$  of each species.

#### **4.3 Constraints of the study**

As none of the investigated traits is related to xylem vulnerability in our dataset, it seems likely, that other determinants are the decisive factor. A vessel trait that has not been assessed in this study is the structure of intervessel pits (Choat et al. 2008). Recent studies suggest, that

there is a strong correlation of pit membrane thickness and xylem vulnerability and that this trait might be the best predictor for xylem vulnerability (Li et al. 2016). Additionally the porosity of pit membranes and their total surface area appear to have an influence in xylem resistance (Wheeler et al. 2005; Jansen et al. 2009). Pit membrane thickness was moreover found to correlate with intervessel wall thickness (Li et al. 2016), which could explain the frequently observed correlation between wood density and xylem vulnerability.

Methodological issues are another possible explanation for the absence of relation of xylem vulnerability in our dataset. Although the bench dehydration method is widely applied in plant hydraulics (Cochard et al. 2013) and considered as a reference method (Longepierre et al. 2014), there is an ongoing discussion about the actual reliability of this method, because of its high susceptibility to artefact introduction (Jansen et al. 2015). A major issue is that the xylem system has to be cut under tension, which was found to introduce embolisms (Wheeler et al. 2013; Torres-Ruiz et al. 2015). However, Longepierre et al. (2014) tested the reliability of the bench dehydration method and found it to be a suitable technique, if sufficient length of branch samples is ensured to avoid an open vessel artefact. In our case, we used the 1.7-fold MVL as the minimum length for our branch samples, which should ensure a sufficient distance between the proximal cut and the distal end of the branch to avoid open vessels. Nevertheless, the measured subsegment was not from the very distal end of the branch, but located in the last third. In addition, MVL showed the highest correlation value with  $P_{50}$ , even if not significant. This might be an indication, that in long vessel species, the measured segment was more likely to fall within the reach of open vessels from the proximal cut.

Besides this, the bench dehydration method is very labor intensive, hence the number of replicates within each tree was limited ( $n = 5$ ). Therefore, it was not possible to construct vulnerability curves for single individuals, which would have yielded a more differentiated view on xylem safety within each species and possibly facilitated the detection of more subtle relationships between xylem anatomy and safety.

#### **4.4 Implications for future species composition**

This study reports the xylem anatomical differences among Sumatran rainforests trees. These traits were found to shape species composition in tropical rainforests in regard to different hydrological conditions (Engelbrecht et al. 2007; Baltzer et al. 2008). Species with low WD, large D and high  $A_{\text{lumen}} : A_{\text{xylem}}$  seem to be more threatened in water restricted habitats (Cosme et al. 2017). This would especially apply to the two *Shorea* species *S. ovalis* and *S. parvifolia*. Both are of economic value for timber production and also inhabit a momentous ecological role as emergent layer species (Kitajima et al. 2005; Nepstad et al. 2007). However, both species also show the widest range of intraspecific variance in those sensible xylem traits, which

implies a high adaption potential (Poorter et al. 2018). This is not the case for species like *P. caerulescens* and *N. kingii*, which have lower traits variability and thus a putative smaller margin for adaption to changing climate.

Additionally, the independency of growth rates and xylem vulnerability indicates, that drought related xylem failure is not yet a growth limiting factor in the Harapan rainforest. This is also visible in the high  $P_{50}$  values of the investigated species and the existence of species with low hydraulic safety and low efficiency. A reduction of water availability would therefore introduce a new selective pressure to this area, which might dramatically alter growth and survival and cause a shift in species composition.

## 5. Conclusion

We investigated the xylem safety as well as xylem anatomical and hydraulic traits of eight Sumatran rainforest tree species. The analyzed traits varied substantially between species, but we did not find any significant correlation with xylem vulnerability. We conclude, that either the main determinant of xylem safety was not assessed in this study or that limits in methodology hindered the compilation of a robust data set. For the first reason, we suggest to include intervessel pit anatomy in future investigations of xylem safety, as this seems to be the most promising predictor. Furthermore, complex traits like wood density and tree height appear to be non-reliable predictors of xylem vulnerability. Their correlation with xylem safety is mediated through xylem anatomical traits, that are scaling with WD or H. Hence, their relationship is of indirect and not causal nature.

Even if no significant negative correlation between xylem vulnerability and  $K_p$  could be found, it seems likely, that there is a trade-off between hydraulic safety and efficiency in the studied species, because none of the investigated species showed a high conductivity and a high xylem safety. Instead, three of the eight species showed a low efficiency and a low safety. Presumably, the perhumid environment causes a weak selective pressure towards xylem safety.

Apart from explicatory aims, this study reports the diversity of xylem anatomical differences among eight Sumatran trees species. Even If a significant influence on xylem vulnerability could not be detected, such xylem anatomical traits were reported to determine species composition in regard to different hydrological conditions in tropical rainforests. Therefore, we can infer that altering precipitation regimes will have heterogenic effects on the performance of different species, subsequently altering the species composition in Sumatran rainforests.

## **Acknowledgement**

Many people contributed to the success of this thesis with scientific support, motivational talks or cheering company. First, I would like to thank Prof. Dr. Christoph Leuschner for the opportunity to work in his department and for granting and reviewing the topic. Despite his numerous duties, he was always reachable for last-minute questions. Further I wish to thank Bernhard Schuldt for acting as my second referee and especially for his continuous support during the writing process. His counseling and conceptual input were a great help for this work. Special thanks go to Pierre-André Waite, for his eminent support during field work. He planned the sampling campaign and organized many things in fluent *bahasa Indonesia*. Also, he took his time to review the manuscript.

Further, I would like to thank Dietrich Hertel for bringing up the idea to apply at this project and for linking me with the persons in charge. I also wish to express my gratitude to Roman Link, who did not only contribute to the statistical analysis, but also helped me to substantially increase my R skills. Many thanks to my assistants in Jambi (Irul, Udin, Tiwi and Vira) for their engaged work and for our unforgettable explorations around Jambi and in the Kerinci mountains.

Finally, I would like to thank my family, especially my mother, and my friends for their unconditional love and friendship. I am looking forward to future adventures with you!

## References

Allen, Craig D.; Breshears, David D.; McDowell, Nate G. (2015): On underestimation of global vulnerability to tree mortality and forest die-off from hotter drought in the Anthropocene. In *Ecosphere* 6 (8), art129. DOI: 10.1890/ES15-00203.1.

Allen, Craig D.; Macalady, Alison K.; Chenchouni, Haroun; Bachelet, Dominique; McDowell, Nate; Vennetier, Michel et al. (2010): A global overview of drought and heat-induced tree mortality reveals emerging climate change risks for forests. In *Forest Ecology and Management* 259 (4), pp. 660–684. DOI: 10.1016/j.foreco.2009.09.001.

Anderegg, William R. L.; Klein, Tamir; Bartlett, Megan; Sack, Lawren; Pellegrini, Adam F. A.; Choat, Brendan; Jansen, Steven (2016): Meta-analysis reveals that hydraulic traits explain cross-species patterns of drought-induced tree mortality across the globe. In *Proceedings of the National Academy of Sciences of the United States of America* 113 (18), pp. 5024–5029. DOI: 10.1073/pnas.1525678113.

Apgaua, Deborah M. G.; Tng, David Y. P.; Cernusak, Lucas A.; Cheesman, Alexander W.; Santos, Rubens M.; Edwards, Will J. et al. (2016): Plant functional groups within a tropical forest exhibit different wood functional anatomy. In *Functional Ecology* 31 (3), pp. 582–591. DOI: 10.1111/1365-2435.12787.

Arnold, Jeffrey B. (2018): ggthemes: Extra Themes, Scales and Geoms for 'ggplot2'. Version R package version 4.0.1. Available online at <https://CRAN.R-project.org/package=ggthemes>.

Auguie, Baptiste (2017): gridExtra: Miscellaneous Functions for "Grid" Graphics. Version R package version 2.3. Available online at <https://CRAN.R-project.org/package=gridExtra>.

Bache, Stefan Milton; Wickham, Hadley (2014): magrittr: A Forward-Pipe Operator for R. Version R package version 1.5. Available online at <https://CRAN.R-project.org/package=magrittr>.

Baltzer, J. L.; Davies, S. J.; Bunyavejchewin, S.; Noor, N. S. M. (2008): The role of desiccation tolerance in determining tree species distributions along the Malay–Thai Peninsula. In *Functional Ecology* 22 (2), pp. 221–231. DOI: 10.1111/j.1365-2435.2007.01374.x.

- Bennett, Amy C.; McDowell, Nathan G.; Allen, Craig D.; Anderson-Teixeira, Kristina J. (2015): Larger trees suffer most during drought in forests worldwide. In *Nature plants* 1, p. 15139. DOI: 10.1038/nplants.2015.139.
- Boehm, Josef (1893): Capillarität und saftsteigen. In *Berichte der Deutschen Botanische Gesellschaft* (11), pp. 203–212.
- Bonan, Gordon B. (2008): Forests and climate change: forcings, feedbacks, and the climate benefits of forests. In *Science (New York, N.Y.)* 320 (5882), pp. 1444–1449. DOI: 10.1126/science.1155121.
- Bond, Barbara J.; Meinzer, Frederick C.; Brooks, Renée J. (2008): How trees influence the hydrological cycle in forest ecosystems. In Paul J. Wood, David M. Hannah, Jonathan P. Sadler (Eds.): *Hydroecology and ecohydrology. Past, present and future*. Repr. Chichester: John Wiley & Sons, pp. 7–35.
- Brown, Harvey R. (2013): The Theory of the Rise of Sap in Trees: Some Historical and Conceptual Remarks. In *Phys. Perspect.* 15 (3), pp. 320–358. DOI: 10.1007/s00016-013-0117-1.
- Brown, James H. (2014): Why are there so many species in the tropics? In *Journal of biogeography* 41 (1), pp. 8–22. DOI: 10.1111/jbi.12228.
- Chave, Jerome; Coomes, David; Jansen, Steven; Lewis, Simon L.; Swenson, Nathan G.; Zanne, Amy E. (2009): Towards a worldwide wood economics spectrum. In *Ecology Letters* 12 (4), pp. 351–366. DOI: 10.1111/j.1461-0248.2009.01285.x.
- Choat, Brendan; Cobb, Alexander R.; Jansen, Steven (2008): Structure and function of bordered pits: new discoveries and impacts on whole-plant hydraulic function. In *The New phytologist* 177 (3), pp. 608–625. DOI: 10.1111/j.1469-8137.2007.02317.x.
- Choat, Brendan; Creek, Danielle; Lo A. Gullo, Maria; Nardini, Andrea; Oddo, Elisabetta; Raimondo, Fabio et al. (2015): Quantification of vulnerability to xylem embolism - Bench dehydration. PrometheusWiki. Available online at [https://www.researchgate.net/publication/282008335\\_PrometheusWiki\\_-\\_Quantification\\_of\\_vulnerability\\_to\\_xylem\\_embolism\\_-\\_Bench\\_dehydration](https://www.researchgate.net/publication/282008335_PrometheusWiki_-_Quantification_of_vulnerability_to_xylem_embolism_-_Bench_dehydration).
- Choat, Brendan; Jansen, Steven; Brodribb, Tim J.; Cochard, Hervé; Delzon, Sylvain; Bhaskar, Radika et al. (2012): Global convergence in the vulnerability of forests to drought. In *Nature* 491, 752 EP -. DOI: 10.1038/nature11688.

Clark, Deborah A. (2004): Sources or sinks? The responses of tropical forests to current and future climate and atmospheric composition. In *Philosophical transactions of the Royal Society of London. Series B, Biological sciences* 359 (1443), pp. 477–491. DOI: 10.1098/rstb.2003.1426.

Cochard, Hervé (2006): Cavitation in trees. In *Comptes Rendus Physique* 7 (9-10), pp. 1018–1026. DOI: 10.1016/j.crhy.2006.10.012.

Cochard, Hervé; Badel, Eric; Herbette, Stéphane; Delzon, Sylvain; Choat, Brendan; Jansen, Steven (2013): Methods for measuring plant vulnerability to cavitation: a critical review. In *Journal of experimental botany* 64 (15), pp. 4779–4791. DOI: 10.1093/jxb/ert193.

Cohen, Shabtai; Bennink, John; Tyree, Mel (2003): Air method measurements of apple vessel length distributions with improved apparatus and theory\*. In *jxb* 54 (389), pp. 1889–1897. DOI: 10.1093/jxb/erg202.

Comstock, Jonathan P.; Sperry, John S. (2000): Theoretical considerations of optimal conduit length for water transport in vascular plants. In *New Phytologist* 148 (2), pp. 195–218. DOI: 10.1046/j.1469-8137.2000.00763.x.

Cosme, Luiza H. M.; Schietti, Juliana; Costa, Flávia R. C.; Oliveira, Rafael S. (2017): The importance of hydraulic architecture to the distribution patterns of trees in a central Amazonian forest. In *New Phytologist* 215 (1), pp. 113–125. DOI: 10.1111/nph.14508.

da Costa, Antonio Carlos Lola; Galbraith, David; Almeida, Samuel; Portela, Bruno Takeshi Tanaka; da Costa, Mauricio; Silva Junior, João de Athaydes et al. (2010): Effect of 7 yr of experimental drought on vegetation dynamics and biomass storage of an eastern Amazonian rainforest. In *The New phytologist* 187 (3), pp. 579–591. DOI: 10.1111/j.1469-8137.2010.03309.x.

D'Almeida, Cassiano; Vörösmarty, Charles J.; Hurtt, George C.; Marengo, José A.; Dingman, S. Lawrence; Keim, Barry D. (2007): The effects of deforestation on the hydrological cycle in Amazonia: a review on scale and resolution. In *Int. J. Climatol.* 27 (5), pp. 633–647. DOI: 10.1002/joc.1475.

Denman, K. L.; G. Brasseur; A. Chidthaisong; P. Ciais, P. CoxM.; R.E. Dickinson; D. Hauglustaine et al. (2007): Couplings Between Changes in the Climate System and Biogeochemistry. In IPCC (Ed.): *Climate Change 2007. The Physical Science Basis. Contribution of Working Group I to the Fourth Assessment Report of the Intergovernmental Panel on Climate Change.* With

assistance of Solomon, S., D. Qin, M. Manning, Z. Chen, M. Marquis, K.B. Averyt, M. Tignor, H.L. Miller. Cambridge, United Kingdom and New York, NY, USA: Cambridge University Press, pp. 499–587.

Dixon, H. H.; Joly, J. (1894): ON THE ASCENT OF SAP. In *Annals of botany* 8 (32), pp. 468–470.

Drescher, Jochen; Rembold, Katja; Allen, Kara; Beckschäfer, Philip; Buchori, Damayanti; Clough, Yann et al. (2016): Ecological and socio-economic functions across tropical land use systems after rainforest conversion. In *Philosophical transactions of the Royal Society of London. Series B, Biological sciences* 371 (1694). DOI: 10.1098/rstb.2015.0275.

Ebeling, Anne; Rzanny, Michael; Lange, Markus; Eisenhauer, Nico; Hertzog, Lionel R.; Meyer, Sebastian T.; Weisser, Wolfgang W. (2018): Plant diversity induces shifts in the functional structure and diversity across trophic levels. In *Oikos* 127 (2), pp. 208–219. DOI: 10.1111/oik.04210.

Engelbrecht, Bettina M. J. (2012): Forests on the brink. In *Nature* 491, 675 EP -. DOI: 10.1038/nature11756.

Engelbrecht, Bettina M. J.; Comita, Liza S.; Condit, Richard; Kursar, Thomas A.; Tyree, Melvin T.; Turner, Benjamin L.; Hubbell, Stephen P. (2007): Drought sensitivity shapes species distribution patterns in tropical forests. In *Nature* 447 (7140), pp. 80–82. DOI: 10.1038/nature05747.

Ewers, Frank W.; Fisher, Jack B. (1989): Techniques for Measuring Vessel Lengths and Diameters in Stems of Woody Plants. In *American journal of botany* 76 (5), p. 645. DOI: 10.2307/2444412.

Fortunel, Claire; Ruelle, Julien; Beauchêne, Jacques; Fine, Paul V. A.; Baraloto, Christopher (2014): Wood specific gravity and anatomy of branches and roots in 113 Amazonian rainforest tree species across environmental gradients. In *New Phytologist* 202 (1), pp. 79–94. DOI: 10.1111/nph.12632.

Gärtner, Holger; Lucchinetti, Sandro; Schweingruber, Fritz (2014): New perspectives for wood anatomical analysis in dendrosciences: The GSL1-microtome. In *Dendrochronologia* 32. DOI: 10.1016/j.dendro.2013.07.002.

Gaviria, Julian; Turner, Benjamin L.; Engelbrecht, Bettina M. J. (2017): Drivers of tree species distribution across a tropical rainfall gradient. In *Ecosphere* 8 (2), e01712. DOI: 10.1002/ecs2.1712.

Giam, Xingli (2017): Global biodiversity loss from tropical deforestation. In *Proceedings of the National Academy of Sciences of the United States of America* 114 (23), pp. 5775–5777. DOI: 10.1073/pnas.1706264114.

Gleason, Sean M.; Westoby, Mark; Jansen, Steven; Choat, Brendan; Hacke, Uwe G.; Pratt, Robert B. et al. (2016): Weak tradeoff between xylem safety and xylem-specific hydraulic efficiency across the world's woody plant species. In *New Phytologist* 209 (1), pp. 123–136. DOI: 10.1111/nph.13646.

Grolemund, Garret; Hadley Wickham (2011): Dates and Times Made Easy with {lubridate}. Available online at <http://www.jstatsoft.org/v40/i03/>.

Groombridge, Brian; Jenkins, Martin D. (2002): World atlas of biodiversity. Earth's living resources in the 21st century. Berkeley, Calif.: Univ. of California Press. Available online at <http://www.loc.gov/catdir/description/ucal042/2002512694.html>.

Guzman, Mark E. de; Santiago, Louis S.; Schnitzer, Stefan A.; Álvarez-Cansino, Leonor (2016): Trade-offs between water transport capacity and drought resistance in neotropical canopy liana and tree species. In *Tree Physiology* 37 (10), pp. 1404–1414. DOI: 10.1093/treephys/tpw086.

Hacke, Uwe G.; Sperry, John S.; Pockman, William T.; Davis, Stephen D.; McCulloh, Katherine A. (2001): Trends in wood density and structure are linked to prevention of xylem implosion by negative pressure. In *Oecologia* 126 (4), pp. 457–461. DOI: 10.1007/s004420100628.

Hadley Wickham (2017): tidyverse: Easily Install and Load the 'Tidyverse'. Version R package version 1.2.1. Available online at <https://CRAN.R-project.org/package=tidyverse>.

Hadley Wickham (2018): scales: Scale Functions for Visualization. Version R package version 1.0.0. Available online at <https://CRAN.R-project.org/package=scales>.

Harrel, Frank E. (2018): Hmisc: Harrell Miscellaneous. Version R package version 4.1-1. Available online at <https://CRAN.R-project.org/package=Hmisc>.

Hietz, Peter; Rosner, Sabine; Hietz-Seifert, Ursula; Wright, S. Joseph (2016): Wood traits related to size and life history of trees in a Panamanian rainforest. In *The New phytologist* 213 (1), pp. 170–180. DOI: 10.1111/nph.14123.

Hoeber, Stefanie; Leuschner, Christoph; Köhler, Lars; Arias-Aguilar, Dagoberto; Schuldt, Bernhard (2014): The importance of hydraulic conductivity and wood

density to growth performance in eight tree species from a tropical semi-dry climate. In *Forest Ecology and Management* 330, pp. 126–136. DOI: 10.1016/j.foreco.2014.06.039.

Hothorn, Torsten; Bretz, Frank; Westfall, Peter (2008): Simultaneous Inference in General Parametric Models.

Huijnen, V.; Wooster, M. J.; Kaiser, J. W.; Gaveau, D. L. A.; Flemming, J.; Parrington, M. et al. (2016): Fire carbon emissions over maritime southeast Asia in 2015 largest since 1997. In *Sci Rep* 6 (1), G04024. DOI: 10.1038/srep26886.

Hunter, M. O.; Keller, M.; Victoria, D.; Morton, D. C. (2013): Tree height and tropical forest biomass estimation. In *Biogeosciences* 10 (12), pp. 8385–8399. DOI: 10.5194/bg-10-8385-2013.

IPCC (Ed.) (2014): Climate Change 2014. Impacts, Adaptation and Vulnerability. Part B: Regional Aspects. Contribution of Working Group II to the Fifth Assessment Report of the Intergovernmental Panel on Climate Change. With assistance of Barros, V.R., C.B. Field, D.J. Dokken, M.D. Mastrandrea, K.J. Mach, T.E. Bilir, M. Chatterjee, K.L. Ebi, Y.O. Estrada, R.C. Genova, B. Girma, E.S. Kissel, A.N. Levy, S. MacCracken, P.R. Mastrandrea, and L.L. White. Cambridge, United Kingdom and New York, NY, USA: Cambridge University Press.

Jansen, Steven; Choat, Brendan; Pletsers, Annelies (2009): Morphological variation of intervessel pit membranes and implications to xylem function in angiosperms. In *American journal of botany* 96 (2), pp. 409–419. DOI: 10.3732/ajb.0800248.

Jansen, Steven; Schuldt, Bernhard; Choat, Brendan (2015): Current controversies and challenges in applying plant hydraulic techniques: International Workshop on Plant Hydraulic Techniques, Ulm University, Germany, September 2014. In *New Phytologist* 205 (3), pp. 961–964. DOI: 10.1111/nph.13229.

Kassambara, Alboukadel (2018): ggpubr: 'ggplot2' Based Publication Ready Plots. Version R package version 0.2. Available online at <https://CRAN.R-project.org/package=ggpubr>.

Kim, Hae Koo; Park, Joonghyuk; Hwang, Ildoo (2014): Investigating water transport through the xylem network in vascular plants. In *Journal of experimental botany* 65 (7), pp. 1895–1904. DOI: 10.1093/jxb/eru075.

- Kitajima, Kaoru; Mulkey, Stephen S.; Wright, S. Joseph (2005): Variation in crown light utilization characteristics among tropical canopy trees. In *Annals of botany* 95 (3), pp. 535–547. DOI: 10.1093/aob/mci051.
- Kotowska, Martyna M.; Hertel, Dietrich; Rajab, Yasmin Abou; Barus, Henry; Schuldt, Bernhard (2015a): Patterns in hydraulic architecture from roots to branches in six tropical tree species from cacao agroforestry and their relation to wood density and stem growth. In *Frontiers in plant science* 6, p. 191. DOI: 10.3389/fpls.2015.00191.
- Kotowska, Martyna M.; Leuschner, Christoph; Triadiati, Triadiati; Meriem, Selis; Hertel, Dietrich (2015b): Quantifying above- and belowground biomass carbon loss with forest conversion in tropical lowlands of Sumatra (Indonesia). In *Global change biology* 21 (10), pp. 3620–3634. DOI: 10.1111/gcb.12979.
- Kunstler, Georges; Falster, Daniel; Coomes, David A.; Hui, Francis; Kooyman, Robert M.; Laughlin, Daniel C. et al. (2016): Plant functional traits have globally consistent effects on competition. In *Nature* 529 (7585), pp. 204–207. DOI: 10.1038/nature16476.
- Lewis, Simon L. (2006): Tropical forests and the changing earth system. In *Philosophical transactions of the Royal Society of London. Series B, Biological sciences* 361 (1465), pp. 195–210. DOI: 10.1098/rstb.2005.1711.
- Li, Shan; Lens, Frederic; Espino, Susana; Karimi, Zohreh; Klepsch, Matthias; Schenk, H. Jochen et al. (2016): INTERVESSEL PIT MEMBRANE THICKNESS AS A KEY DETERMINANT OF EMBOLISM RESISTANCE IN ANGIOSPERM XYLEM. In *IAWA Journal* 37 (2), pp. 152–171. DOI: 10.1163/22941932-20160128.
- Longepierre, D.; Joffre, R.; Martin-StPaul, N. K.; Rambal, S.; Huc, R.; Burlett, R. et al. (2014): How reliable are methods to assess xylem vulnerability to cavitation? The issue of 'open vessel' artifact in oaks. In *treephys* 34 (8), pp. 894–905. DOI: 10.1093/treephys/tpu059.
- Ma, Zhihai; Lei, Xd; Zhu, Qiuhan; Chen, Huai; Wang, Weifeng; Liu, Shirong et al. (2011): A drought-induced pervasive increase in tree mortality across Canada's boreal forests. In *Nature Climate Change* 1. DOI: 10.1038/nclimate1293.
- Margono, Belinda Arunarwati; Turubanova, Svetlana; Zhuravleva, Ilona; Potapov, Peter; Tyukavina, Alexandra; Baccini, Alessandro et al. (2012): Mapping and monitoring deforestation and forest degradation in Sumatra

(Indonesia) using Landsat time series data sets from 1990 to 2010. In *Environ. Res. Lett.* 7 (3), p. 34010. DOI: 10.1088/1748-9326/7/3/034010.

Meir, Patrick; Mencuccini, Maurizio; Dewar, Roderick C. (2015): Drought-related tree mortality: addressing the gaps in understanding and prediction. In *The New phytologist* 207 (1), pp. 28–33. DOI: 10.1111/nph.13382.

Miettinen, Jukka; Hooijer, Aljosja; Shi, Chenghua; Tollenaar, Daniel; Vernimmen, Ronald; Liew, Soo Chin et al. (2012): Extent of industrial plantations on Southeast Asian peatlands in 2010 with analysis of historical expansion and future projections. In *Glob. Change Biol. Bioenergy* 4 (6), pp. 908–918. DOI: 10.1111/j.1757-1707.2012.01172.x.

Nardini, Andrea; Dimasi, Federica; Klepsch, Matthias; Jansen, Steven (2012): Ion-mediated enhancement of xylem hydraulic conductivity in four *Acer* species: relationships with ecological and anatomical features. In *Tree Physiology* 32 (12), pp. 1434–1441. DOI: 10.1093/treephys/tps107.

Nardini, Andrea; Savi, Tadeja; Trifilò, Patrizia; Lo Gullo, Maria A. (2018): Drought Stress and the Recovery from Xylem Embolism in Woody Plants. In Francisco M. Cánovas, Ulrich Lüttge, Rainer Matyssek (Eds.): *Progress in Botany Vol. 79*, vol. 79. Cham: Springer International Publishing (Progress in Botany), pp. 197–231.

Nepstad, Daniel C.; Tohver, Ingrid Marisa; Ray, David; Moutinho, Paulo; Cardinot, Georgina (2007): Mortality of large trees and lianas following experimental drought in Amazon forest. In *Ecology* 88 (9), pp. 2259–2269. DOI: 10.1890/06-1046.1.

Ogle, Kiona; Barber, Jarrett J.; Willson, Cynthia; Thompson, Brenda (2009): Hierarchical statistical modeling of xylem vulnerability to cavitation. In *New Phytologist* 182 (2), pp. 541–554. DOI: 10.1111/j.1469-8137.2008.02760.x.

Olson, Mark E.; Anfodillo, Tommaso; Rosell, Julieta A.; Petit, Gai; Crivellaro, Alan; Isnard, Sandrine et al. (2014): Universal hydraulics of the flowering plants: vessel diameter scales with stem length across angiosperm lineages, habits and climates. In *Ecology Letters* 17 (8), pp. 988–997. DOI: 10.1111/ele.12302.

Pan, Yude; Birdsey, Richard A.; Phillips, Oliver L.; Jackson, Robert B. (2013): The Structure, Distribution, and Biomass of the World's Forests. In *Annu. Rev. Ecol. Evol. Syst.* 44 (1), pp. 593–622. DOI: 10.1146/annurev-ecolsys-110512-135914.

Parolin, Pia; Worbes, Martin (2000): Wood density of trees in black water floodplains of Rio Jaú National Park, Amazonia, Brazil. In *Acta Amazonica* 30 (3), pp. 441–448.

Pérez-Harguindeguy, N.; Díaz, S.; Garnier, E.; Lavorel, S.; Poorter, H.; Jaureguiberry, P. et al. (2013): New handbook for standardised measurement of plant functional traits worldwide. In *Aust. J. Bot.* 61 (3), p. 167. DOI: 10.1071/BT12225.

Phillips, Oliver L.; van der Heijden, Geertje; Lewis, Simon L.; López-González, Gabriela; Aragão, Luiz E. O. C.; Lloyd, Jon et al. (2010): Drought-mortality relationships for tropical forests. In *New Phytologist* 187 (3), pp. 631–646. DOI: 10.1111/j.1469-8137.2010.03359.x.

Poorter, Lourens; Castilho, Carolina V.; Schiatti, Juliana; Oliveira, Rafael S.; Costa, Flávia R. C. (2018): Can traits predict individual growth performance? A test in a hyperdiverse tropical forest. In *New Phytologist* 219 (1), pp. 109–121. DOI: 10.1111/nph.15206.

Poorter, Lourens; McDonald, Imole; Alarcón, Alfredo; Fichtler, Esther; Licona, Juan-Carlos; Peña-Claros, Marielos et al. (2010): The importance of wood traits and hydraulic conductance for the performance and life history strategies of 42 rainforest tree species. In *The New phytologist* 185 (2), pp. 481–492. DOI: 10.1111/j.1469-8137.2009.03092.x.

Powell, Thomas L.; Wheeler, James K.; Oliveira, Alex A. R. de; da Costa, Antonio Carlos Lola; Saleska, Scott R.; Meir, Patrick; Moorcroft, Paul R. (2017): Differences in xylem and leaf hydraulic traits explain differences in drought tolerance among mature Amazon rainforest trees. In *Global change biology* 23 (10), pp. 4280–4293. DOI: 10.1111/gcb.13731.

Preston, Katherine A.; Cornwell, William K.; Denoyer, Jeanne L. (2006): Wood density and vessel traits as distinct correlates of ecological strategy in 51 California coast range angiosperms. In *The New phytologist* 170 (4), pp. 807–818. DOI: 10.1111/j.1469-8137.2006.01712.x.

R Core Team (2018): R: A language and environment for statistical computing. Version 3.5.0. Vienna, Austria: R Foundation for Statistical Computing. Available online at <https://www.R-project.org/>.

Rejou-Mechain, Maxime; Tanguy, Ariane; Piponiot, Camille; Chave, Jerome; Herault, Bruno (2018): BIOMASS. Estimating Aboveground Biomass and Its Uncertainty in Tropical Forests. R package. Version 1.2.

Revelle, William (2018): psych: Procedures for Psychological, Psychometric, and Personality Research. Version R package version 1.8.4. Available online at <https://CRAN.R-project.org/package=psych>.

Rind, D. (2013): The influence of vegetation on the hydrologic cycle in a global climate model. In James E. Hansen, Taro Takahashi (Eds.): *Climate Processes and Climate Sensitivity*, vol. 29. 235 volumes. Washington, D. C.: American Geophysical Union (Geophysical Monograph Series, 29), pp. 73–91.

Roberts, J. M. (2009): The role of forests in the hydrological cycle. In John N. Owens, H. Gyde Lund (Eds.): *Forests and forest plants*. Vol. 3. 3 volumes. Oxford, UK: Eolss Publishers Co Ltd, pp. 42–76.

Robinson, David; Hayes, Alex (2018): broom: Convert Statistical Analysis Objects into Tidy Tibbles. Version R package version 0.5.0. Available online at <https://CRAN.R-project.org/package=broom>.

Rockwell, Fulton E.; Wheeler, James K.; Holbrook, N. Michele (2014): Cavitation and its discontents: opportunities for resolving current controversies. In *Plant Physiol* 164 (4), pp. 1649–1660. DOI: 10.1104/pp.113.233817.

Rouvinen, Seppo; Kuuluvainen, Timo; Siitonen, Juha (2002): Tree Mortality in a *Pinus sylvestris* Dominated Boreal Forest Landscape in Vienansalo Wilderness, Eastern Fennoscandia. In *Silva Fenn.* 36 (1). DOI: 10.14214/sf.554.

Rowland, L.; da Costa, A. C. L.; Galbraith, D. R.; Oliveira, R. S.; Binks, O. J.; Oliveira, A. A. R. et al. (2015): Death from drought in tropical forests is triggered by hydraulics not carbon starvation. In *Nature* 528 (7580), pp. 119–122. DOI: 10.1038/nature15539.

Santiago, L. S.; Goldstein, G.; Meinzer, F. C.; Fisher, J. B.; Machado, K.; Woodruff, D.; Jones, T. (2004): Leaf photosynthetic traits scale with hydraulic conductivity and wood density in Panamanian forest canopy trees. In *Oecologia* 140 (4), pp. 543–550. DOI: 10.1007/s00442-004-1624-1.

Scherber, Christoph; Eisenhauer, Nico; Weisser, Wolfgang W.; Schmid, Bernhard; Voigt, Winfried; Fischer, Markus et al. (2010): Bottom-up effects of plant diversity on multitrophic interactions in a biodiversity experiment. In *Nature* 468 (7323), pp. 553–556. DOI: 10.1038/nature09492.

- Scholander, P. F.; Hammel, H. T.; Hemmingsen, E. A.; Bradstreet, E. D. (1964): Hydrostatic pressure and osmotic potential in leaves of mangroves and some other plants. In *Proceedings of the National Academy of Sciences of the United States of America* 52 (1), pp. 119–125.
- Schuldt, Bernhard; Leuschner, Christoph; Brock, Nicolai; Horna, Viviana (2013): Changes in wood density, wood anatomy and hydraulic properties of the xylem along the root-to-shoot flow path in tropical rainforest trees. In *Tree Physiology* 33 (2), pp. 161–174. DOI: 10.1093/treephys/tps122.
- Skene, D. S.; Balodis, V. (1968): A Study of Vessel Length in *Eucalyptus obliqua* L'Hérit. In *jxb* 19 (4), pp. 825–830. DOI: 10.1093/jxb/19.4.825.
- Sperry, J. S.; Donnelly, J. R.; Tyree, M. T. (1988): A method for measuring hydraulic conductivity and embolism in xylem. In *Plant Cell Environ* 11 (1), pp. 35–40. DOI: 10.1111/j.1365-3040.1988.tb01774.x.
- Sperry, J. S.; Tyree, M. T. (1988): Mechanism of Water Stress-Induced Xylem Embolism. In *Plant Physiology* 88 (3), pp. 581–587. DOI: 10.1104/pp.88.3.581.
- Sperry, John S.; Hacke, U. G.W.E.; Wheeler, James K. (2005): Comparative analysis of end wall resistivity in xylem conduits. In *Plant Cell Environ* 28 (4), pp. 456–465. DOI: 10.1111/j.1365-3040.2005.01287.x.
- Sperry, John S.; Meinzer, Frederick C.; McCulloh, Katherine A. (2008): Safety and efficiency conflicts in hydraulic architecture: scaling from tissues to trees. In *Plant, Cell & Environment* 31 (5), pp. 632–645. DOI: 10.1111/j.1365-3040.2007.01765.x.
- Sperry, John S.; Nichols, Kirk L.; Sullivan, June E. M.; Eastlack, Sonda E. (1994): Xylem Embolism in Ring-Porous, Diffuse-Porous, and Coniferous Trees of Northern Utah and Interior Alaska. In *Ecology* 75 (6), pp. 1736–1752. DOI: 10.2307/1939633.
- Torres-Ruiz, José M.; Jansen, Steven; Choat, Brendan; McElrone, Andrew J.; Cochard, Hervé; Brodribb, Timothy J. et al. (2015): Direct x-ray microtomography observation confirms the induction of embolism upon xylem cutting under tension. In *Plant Physiol* 167 (1), pp. 40–43. DOI: 10.1104/pp.114.249706.
- Tyree, M. T.; Sperry, J. S. (1989): Vulnerability of Xylem to Cavitation and Embolism. In *Annual Review of Plant Physiology and Plant Molecular Biology* 40 (1), pp. 19–36. DOI: 10.1146/annurev.pp.40.060189.000315.

- Tyree, M. T.; Zimmermann, Martin Huldrych (2002): Xylem structure and the ascent of sap. 2nd ed. Berlin: Springer.
- Tyree, Melvin T. (2003): Plant hydraulics: the ascent of water. In *Nature* 423 (6943), p. 923. DOI: 10.1038/423923a.
- van der Sande, Masha T.; Poorter, Lourens; Schnitzer, Stefan A.; Engelbrecht, Bettina M. J.; Markesteijn, Lars (2019): The hydraulic efficiency-safety trade-off differs between lianas and trees. In *Ecology*, e02666. DOI: 10.1002/ecy.2666.
- van Mantgem, Phillip J.; Stephenson, Nathan L. (2007): Apparent climatically induced increase of tree mortality rates in a temperate forest. In *Ecology Letters* 10 (10), pp. 909–916. DOI: 10.1111/j.1461-0248.2007.01080.x.
- Wheeler, James K.; Huggett, Brett A.; Tofte, Alena N.; Rockwell, Fulton E.; Holbrook, N. Michele (2013): Cutting xylem under tension or supersaturated with gas can generate PLC and the appearance of rapid recovery from embolism. In *Plant Cell Environ* 36 (11), pp. 1938–1949. DOI: 10.1111/pce.12139.
- Wheeler, James K.; Sperry, John S.; Hacke, U. G.W.E.; Hoang, Nguyen (2005): Inter-vessel pitting and cavitation in woody Rosaceae and other vesselled plants: a basis for a safety versus efficiency trade-off in xylem transport. In *Plant, Cell and Environment* 28 (6), pp. 800–812. DOI: 10.1111/j.1365-3040.2005.01330.x.
- White, F. M. (1991): Viscous fluid flow. New York: McGraw-Hill.
- Wickham, Hadley; Henry, Lionel (2018): tidy: Easily Tidy Data with 'spread' and 'gather' Functions. Version R package version 0.8.1. Available online at <https://CRAN.R-project.org/package=tidy>.
- Youngentob, Kara N.; Zdenek, Christina; van Gorsel, Eva (2016): A simple and effective method to collect leaves and seeds from tall trees. In *Methods in Ecology and Evolution* 7 (9), pp. 1119–1123. DOI: 10.1111/2041-210X.12554.
- Zach, Alexandra; Schuldt, Bernhard; Brix, Sarah; Horna, Viviana; Culmsee, Heike; Leuschner, Christoph (2010): Vessel diameter and xylem hydraulic conductivity increase with tree height in tropical rainforest trees in Sulawesi, Indonesia. In *Flora - Morphology, Distribution, Functional Ecology of Plants* 205 (8), pp. 506–512. DOI: 10.1016/j.flora.2009.12.008.
- Zanne, Amy E.; Westoby, Mark; Falster, Daniel S.; Ackerly, David D.; Loarie, Scott R.; Arnold, Sarah E. J.; Coomes, David A. (2010): Angiosperm wood structure: Global patterns in vessel anatomy and their relation to wood density

and potential conductivity. In *American journal of botany* 97 (2), pp. 207–215. DOI: 10.3732/ajb.0900178.

Zhang, Yong-Jiang; Meinzer, Frederick C.; Hao, Guang-You; Scholz, Fabian G.; Bucci, Sandra J.; Takahashi, Frederico S. C. et al. (2009): Size-dependent mortality in a Neotropical savanna tree: the role of height-related adjustments in hydraulic architecture and carbon allocation. In *Plant, Cell & Environment* 32 (10), pp. 1456–1466. DOI: 10.1111/j.1365-3040.2009.02012.x.

Ziemińska, Kasia; Butler, Don W.; Gleason, Sean M.; Wright, Ian J.; Westoby, Mark (2013): Fibre wall and lumen fractions drive wood density variation across 24 Australian angiosperms. In *AoB PLANTS* 5, p. 25. DOI: 10.1093/aobpla/plt046.

Ziemińska, Kasia; Westoby, Mark; Wright, Ian J. (2015): Broad Anatomical Variation within a Narrow Wood Density Range--A Study of Twig Wood across 69 Australian Angiosperms. In *PloS one* 10 (4), e0124892. DOI: 10.1371/journal.pone.0124892.

Zwieniecki, M. A.; Melcher, P. J.; Michele Holbrook, N. M. (2001): Hydrogel control of xylem hydraulic resistance in plants. In *Science (New York, N.Y.)* 291 (5506), pp. 1059–1062. DOI: 10.1126/science.1057175.

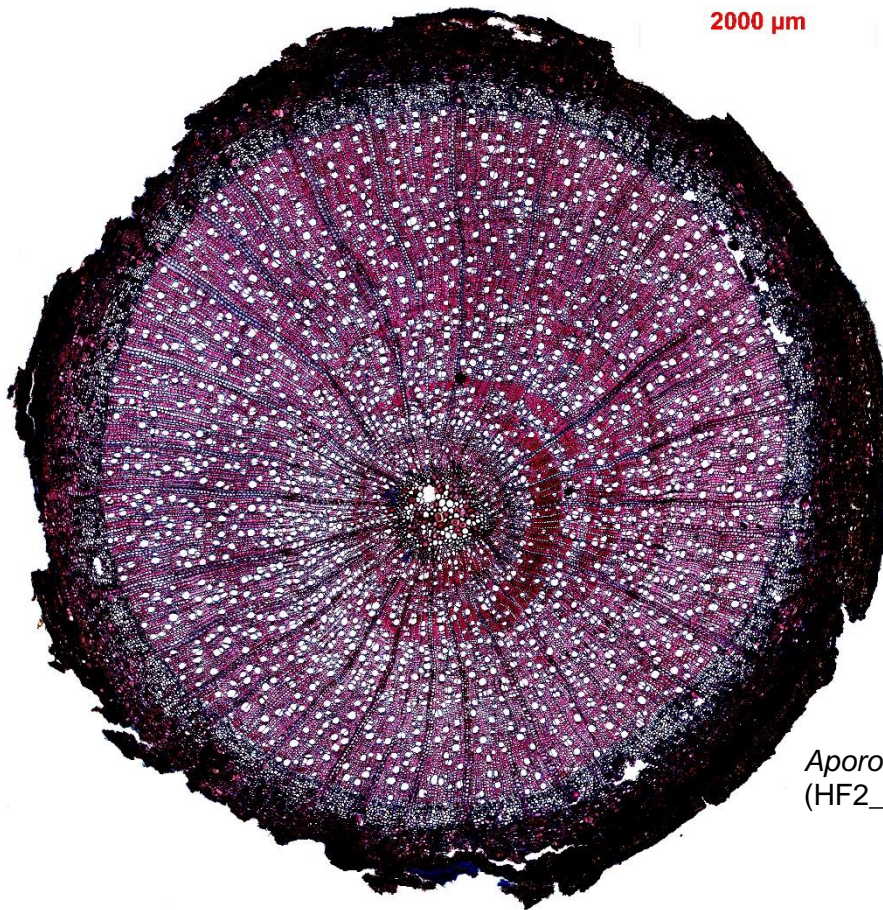
## Appendix

Appendix 1: Aboveground biomass (AGB) and underlying variables for each investigated tree. AGB increment: n.s. indicates non-significance ( $p > 0.05$ ), if no p-value is given:  $p < 0.01$ . Letters in brackets after species names indicate significant differences in the AGB and annual growth (%) between species (ANOVA  $p \leq 0.05$ , Tukey).

Tree ID	Species	Trunk diameter (cm)	AGB (kg)	AGB increment (kg year <sup>-1</sup> )	AGB increment (%)	Tree height (m)	Wood density (g cm <sup>-3</sup> )
HF1_02866		12.74	80.90	5.28	6.50	14.70	0.60
HF1_02905	<i>Aporosa nervosa</i> (ab, a)	17.35	154.30	3.73	2.40	16.90	0.55
HF4_03193		23.21	320.70	0.00 (p = ns)	0.00	21.70	0.50
HF2_03611		15.45	151.40	2.85	1.90	15.80	0.72
HF2_03670		16.76	185.60	0.62	0.30	17.70	0.67
HF1_02887	<i>Gynotroches axillaris</i> (ab, a)	21.75	329.00	24.09	7.30	22.30	0.57
HF4_03119		17.18	121.60	4.30	3.50	16.80	0.44
HF4_03128		13.06	67.90	1.74	2.60	16.50	0.43
HF4_03224		33.80	778.90	8.33	1.10	26.40	0.48
HF2_03730		33.32	867.10	8.31	1.00	23.10	0.63
HF3_02938	<i>Koompassia malaccensis</i> (b, b)	30.96	1262.80	73.67	5.80	29.30	0.85
HF4_03107		80.18	12277.10	190.77	1.60	48.20	0.79
HF4_03170		44.27	3197.60	62.99	2.00	37.30	0.85
HF2_03609		24.60	671.60	12.28	1.80	24.30	0.85
HF3_03004	<i>Neoscortechinia kingii</i> (a, a)	11.08	66.90	1.14	1.70	13.30	0.72
HF4_03136		14.45	168.00	2.31	1.40	20.10	0.72
HF4_03142		16.74	183.10	2.78	1.50	18.60	0.63
HF2_03659		10.77	60.50	1.71	2.80	12.70	0.72
HF2_03738		20.57	303.80	3.46	1.10	18.20	0.72
HF1_02861	<i>Pternandra caerulescens</i> (ab, a)	26.54	502.10	13.15	2.60	24.20	0.55
HF3_02962		11.01	58.70	0.39	0.70	15.60	0.55
HF3_03053		13.46	64.60	4.48	6.90	12.50	0.50
HF2_03682		41.48	931.50	14.76	1.60	22.50	0.45
HF2_03704		30.11	588.10	17.39	3.00	21.10	0.57
HF1_02784	<i>Santiria apiculata</i> (ab, a)	56.90	3637.20	76.62	2.10	35.60	0.61
HF3_02956		13.22	96.60	2.82	2.90	17.20	0.57
HF3_03071		46.69	1666.10	12.00	0.70	27.90	0.52
HF2_03672		21.95	334.60	22.27	6.70	21.20	0.60
HF2_03758		17.78	155.00	7.48	4.80	13.90	0.63
HF3_03012	<i>Shorea ovalis</i> (ab, a)	52.65	2372.70	34.22	1.40	36.40	0.45
HF3_03041		43.14	1346.10	1.07 (p = ns)	0.10	35.80	0.38
HF4_03169		34.96	888.90	22.81	2.60	23.90	0.57
HF2_03665		60.41	2382.60	40.86	1.70	32.10	0.39
HF2_03748		14.00	61.10	2.02	3.30	15.00	0.37
HF1_02812	<i>Shorea parvifolia</i> (ab, a)	20.47	131.00	10.12	7.70	16.60	0.34
HF3_02973		46.37	1517.20	37.63	2.50	32.80	0.41
HF3_03066		57.27	3583.90	21.61	0.60	41.20	0.52
HF4_03179		22.57	196.20	10.47	5.30	21.10	0.33
HF2_03771		12.33	62.20	0.80	1.30	17.40	0.41

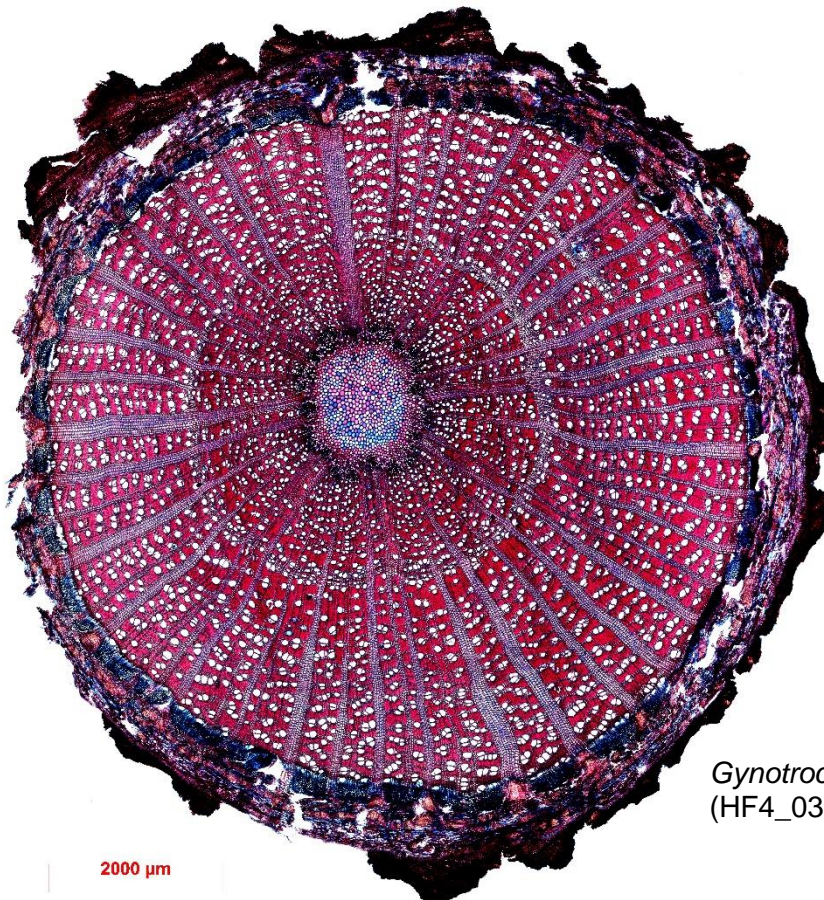
Appendix 2: Median values per species of the investigated xylem anatomical and hydraulic traits.

	<b>VD (n mm<sup>-1</sup>)</b>	<b>D (µm)</b>	<b>D<sub>h</sub> (µm)</b>	<b>K<sub>s</sub><sup>theo</sup></b>	<b>MVL (cm)</b>	<b>A<sub>lumen</sub> : A<sub>xylem</sub> (%)</b>
<b>Aner</b>	70.5	45.2	52.1	9.0	37.0	12.5
<b>Gaxi</b>	56.9	47.9	58.9	11.0	39.2	11.5
<b>Kmal</b>	34.6	56.3	71.7	17.5	20.5	11.5
<b>Nkin</b>	65.2	38.6	52.9	5.9	9.7	8.4
<b>Pcae</b>	60.8	44.0	55.6	8.1	49.5	10.1
<b>Sapi</b>	97.2	33.6	45.4	5.6	22.6	10.6
<b>Sova</b>	83.5	45.7	62.5	21.7	60.0	22.1
<b>Spar</b>	58.7	49.8	71.5	17.8	48.0	13.4



2000  $\mu$ m

*Aporosa nervosa*  
(HF2\_03670)



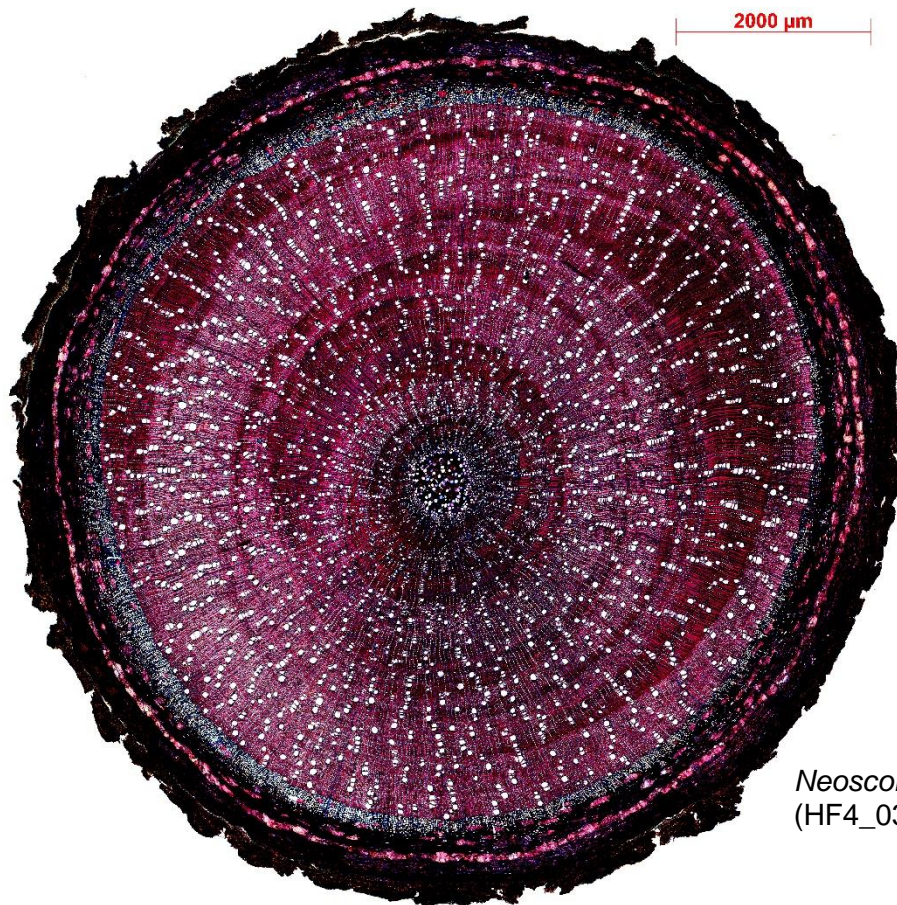
2000  $\mu$ m

*Gynotroches axillaris*  
(HF4\_03224)

Appendix 3: Examples of branch anatomy pictures of *Aporosa nervosa* and *Gynotroches axillaris*. Transverse sections through canopy branches of about 1 cm thickness. Tree ID in brackets.

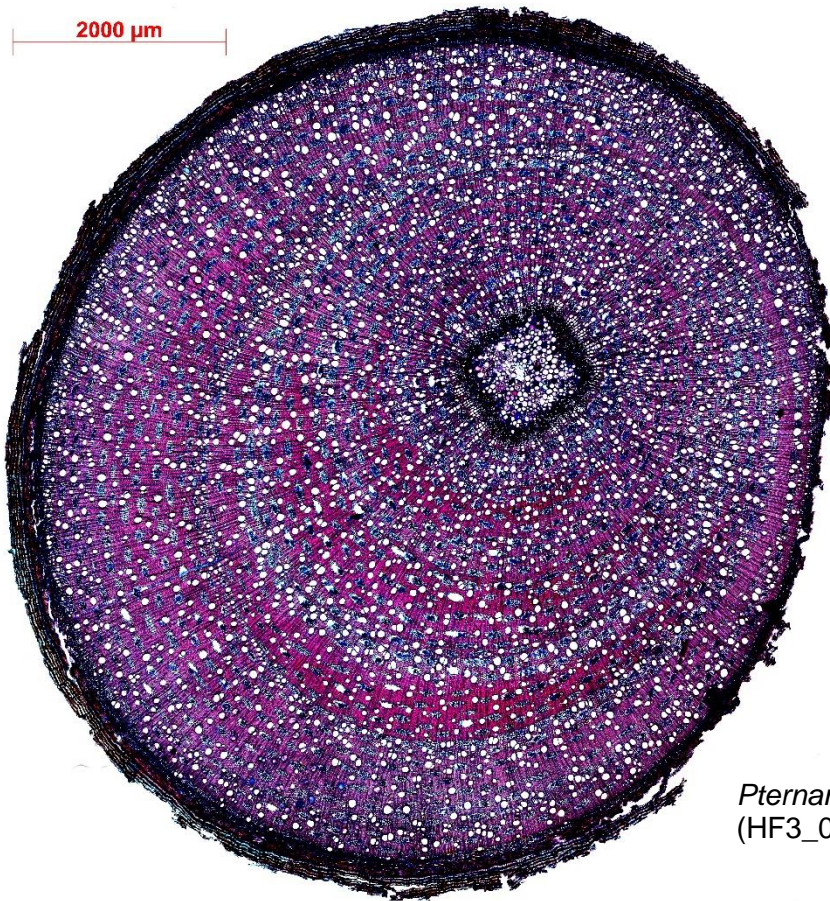


*Koompassia malaccensis*  
(HF2\_03609)



*Neoscortechinia kingii*  
(HF4\_03136)

Appendix 4: Examples of branch anatomy pictures of *Koompassia malaccensis* and *Neoscortechinia kingii*. Transverse sections through canopy branches of about 1 cm thickness. Tree ID in brackets.



*Pternandra caerulescens*  
(HF3\_03053)



*Santiria apiculata*  
(HF2\_03758)

Appendix 5: Examples of branch anatomy pictures of *Pternandra caerulescens* and *Santiria apiculata*. Transverse sections through canopy branches of about 1 cm thickness. Tree ID in brackets.



*Shorea ovalis*  
HF4\_03169



*Shorea parvifolia*  
(HF4\_03179)

Appendix 6: Examples of branch anatomy pictures of *Shorea ovalis* and *Shorea parvifolia*. Transverse sections through canopy branches of about 1 cm thickness. Tree ID in brackets.

Appendix 7: Statistic of vulnerability curves and  $P_{50}$  values.

<b>Species</b>	<b><math>P_{50}</math></b>	<b>SD</b>	<b>p value</b>	<b>t value</b>	<b>Slope</b>	<b>SD</b>	<b>p value</b>	<b>t value</b>
<i>Aporosa nervosa</i>	-1.72	0.49	0.002	-3.52	14.31	8.09	0.092	1.77
<i>Gynotroches axillaris</i>	-1.51	0.19	0.000	-7.76	23.01	7.33	0.005	3.14
<i>Koompassia malaccensis</i>	-2.25	0.24	0.000	-9.37	38.61	20.08	0.071	1.92
<i>Neoscortechinia kingii</i>	-2.76	0.19	0.000	-14.24	32.71	8.28	0.001	3.95
<i>Pternandra caerulescens</i>	-2.59	0.24	0.000	-10.86	23.65	6.52	0.001	3.63
<i>Santiria apiculata</i>	-1.30	0.12	0.000	-10.54	50.14	12.92	0.001	3.88
<i>Shorea ovalis</i>	-1.62	0.21	0.000	-7.80	22.12	7.14	0.005	3.10
<i>Shorea parvifolia</i>	-1.68	0.18	0.000	-9.20	30.90	9.32	0.003	3.31

**Declaration of independent work**

I hereby confirm that I have written the attached thesis on my own and that I did not use any resources than those specified above. This work has not been previously submitted, either in the same or in a similar form to any other examination committee and has not yet been published.

\_\_\_\_\_  
Place, Date

\_\_\_\_\_  
Signature